

AD-A073 145

SRI INTERNATIONAL MENLO PARK CA MOLECULAR PHYSICS LAB
TWO-BODY POSITIVE ION-NEGATIVE ION NEUTRALIZATION. (U)

JAN 79 T M MILLER, A P HICKMAN, F T SMITH

F19628-75-C-0050

F/G 4/1

UNCLASSIFIED

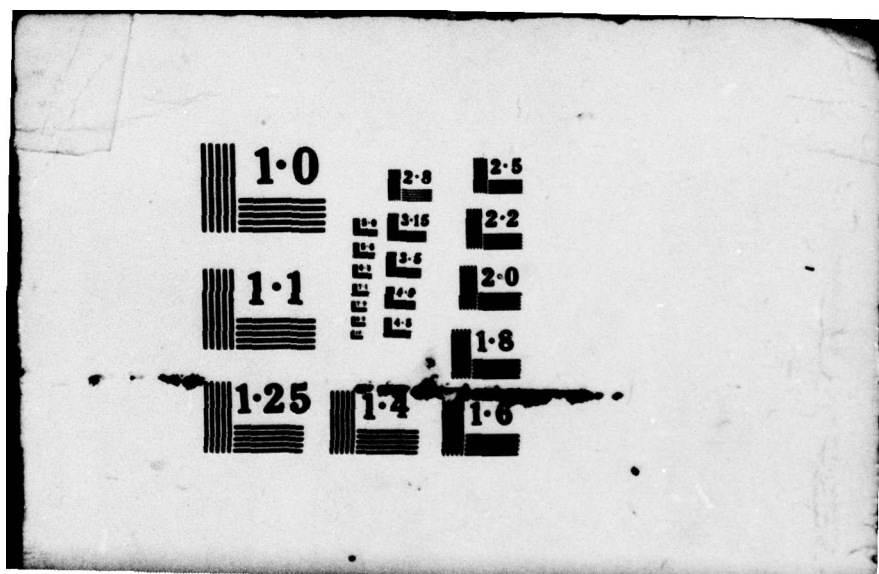
SRI-MP-79-010

AFGL-TR-79-0039

NL

OF
AD
A073 45







Unclassified

SECURITY CLASSIFICATION OF THIS PAGE (When Data Entered)

REPORT DOCUMENTATION PAGE		READ INSTRUCTIONS BEFORE COMPLETING FORM
1. REPORT NUMBER AFGL-TR-79-0039	2. GOVT ACCESSION NO.	3. RECIPIENT'S CATALOG NUMBER
4. TITLE (and Subtitle) TWO-BODY POSITIVE ION-NEGATIVE ION NEUTRALIZATION	5. TYPE OF REPORT & PERIOD COVERED Final Report 10/19/74 to 12/31/78	
6. AUTHOR(S) T. M. Miller, A. P. Hickman, F. T. Smith J. R. Peterson	7. PERFORMING ORGANIZATION NAME AND ADDRESS SRI International 333 Ravenswood Avenue Menlo Park, CA 94025	
8. PERFORMING ORGANIZATION NAME AND ADDRESS Air Force Geophysics Laboratory Hanscom AFB, Massachusetts 01731 Monitor/John Paulson/LKB	9. PROGRAM ELEMENT, PROJECT, TASK AREA & WORK UNIT NUMBERS CDNA01AK	
10. CONTROLLING OFFICE NAME AND ADDRESS Air Force Geophysics Laboratory Hanscom AFB, Massachusetts 01731 Monitor/John Paulson/LKB	11. REPORT DATE 30 Jan 1979	
12. MONITORING AGENCY NAME & ADDRESS (if different from Controlling Office) 627044	13. NUMBER OF PAGES 81	
14. DISTRIBUTION STATEMENT (of this Report) Approved for public release; distribution unlimited	15. SECURITY CLASS. (of this report) Unclassified	
16. SUPPLEMENTARY NOTES This research was sponsored by the Defense Nuclear Agency under Subtask S99QAXHD010, Reaction Rates Critical to Propagation, Work Unit 65, entitled "Measurements of Rate Coefficients for Two-Body Positive" (Continued on back)	17. DISTRIBUTION STATEMENT (of the abstract entered in Block 10, if different from Report) Final rep't. 19 Oct 74- 31 Dec 78	
18. KEY WORDS (Continue on reverse side if necessary and identify by block number) two-body ion-ion neutralization neutralization reaction rate electron transfer complex potential	hydrated ions tidal distortion semiclassical perturbation scattering theory	
19. ABSTRACT (Continue on reverse side if necessary and identify by block number) The results are presented of a combined experimental and theoretical investigation of ion-ion mutual neutralization processes relevant to the earth's ionosphere. Experimental results from our merged beams apparatus (thermal rate coefficients deduced from cross sections for nineteen sets of reactants) and also those from the more recent Birmingham experiments using a flowing afterglow are reviewed. The advantages and disadvantages of both techniques are discussed. A discrepancy in the $\text{NO}_2^{(+)} + \text{NO}_3^{(-)}$ results is		

18. Ion-Negative Ion Neutralization Reactions," and under Subtask S99QAXHD028, Theoretical Studies of Ionizing Mechanisms in the Upper Atmosphere, Work Unit 32, entitled "Theoretical Aspects of the SRI Ion-Ion Laboratory Measurements".

20. attributed to an effect of excitation in the NO_3^- beams of the merged beams, and it is concluded that because of these effects the flowing afterglow is presently better for obtaining rate coefficients for complex molecular ions.

Our theoretical work has focused on two neutralization mechanisms: electron transfer and tidal distortion. A new formulation of the collision dynamics, Semiclassical Perturbation Scattering Theory, was developed and used to estimate the importance of the tidal distortion mechanism. It is concluded that the electron transfer mechanism dominates in reactions of simple ions and small clusters, but that the tidal distortion becomes more important for multiply hydrated reactants. An approximate scaling formula for the rate constants is obtained that fits a wide range of experimental data involving simple ions and small clusters with an accuracy of about $\pm 30\%$.

+ o² -

PREFACE

This Final Report covers work done under contract F19628-75-C-0050, which has been a combined theoretical and experimental study of mutual neutralization reactions between positive and negative ions. These reactions are responsible for the final removal of ions, terminating a long series of ion-neutral reactions that follow the initial ionization and subsequent negative ion formation in the D- and sub-D regions of the earth's ionosphere. Thus they must be included in modeling the ion chemistry of the ionosphere, and they play a particularly sensitive role in those models devoted to VLF and ELF communications problems. Unfortunately, those reaction rates pertinent to the VLF and ELF problems are not yet determined with the desired accuracy and reliability; however, we have determined that the existing experimental facilities at SRI are not capable of substantial improvement toward that end.

Because this report covers the completion of the SRI work using the merged-beam technique, and no further experimental work is contemplated, we take this opportunity to review and summarize all experimental and theoretical work done to date, including experiments at other laboratories. This report thus serves as an up-to-date compilation and review of results on two-body reaction rates. Three-body rates are briefly discussed because of their importance at low altitudes.

Accession For	
NTIS	GR&I
DDC TAB	<input checked="" type="checkbox"/>
Unannounced	<input type="checkbox"/>
Justification	
By _____	
Distribution/	
Availability Codes	
Dist	Avail and/or special
A	

CONTENTS

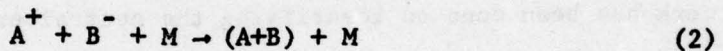
PREFACE	iii
I INTRODUCTION	1
II EXPERIMENTAL TECHNIQUES AND RESULTS	5
A. Measurements of Gases	5
B. Merged-Beams Technique	6
C. Flowing Afterglow Technique	7
III THEORY	17
IV ATMOSPHERIC IMPLICATIONS	23
V FUTURE WORK	25
REFERENCES	27
APPENDICES	29
A. Mutual Neutralization of Simple and Clustered Positive and Negative Ions	31
B. A Laboratory Study of the Reactions of N^+ , N_2^+ , N_3^+ , N_4^+ , O^+ , O_2^+ and NO^+ Ions with Several Molecules at 300 K	33
C. Semiclassical Perturbation Scattering by a Rigid Dipole	35
D. Semiclassical Perturbation Theory of Electron-Molecule Collisions	37
E. Semiclassical Perturbation Theory of Electron- Polar-Molecule Collisions: Total Excitation and Scattering Cross Sections	39
F. Momentum Transfer in Electron-Polar-Molecule Collisions: Results of Semiclassical Perturbation Scattering Theory	41
G. Approximate Scaling Formula for Ion-Ion Mutual Neutralization Rates	43

INTRODUCTION

In this report, we will discuss recent advances in the measurement and calculation of reaction rate coefficients for the positive-ion-negative-ion mutual neutralization process



which has important effects on atmospheric ionization. In reaction (1), A^+ and B^- may be molecular ions, and the neutral products may be excited, dissociated, or rearranged; very little is known about the final products. The corresponding three-body mutual neutralization reaction,



is important at gas pressures greater than a few torr (at altitudes of less than 40 km).

Eq. (1) is of current interest in the chemical modeling of the ionosphere, particularly in the D-region, because it is the final step that removes ionization. The three-body reaction (2) is important in the stratosphere. Three-body mutual neutralization has long been studied in regard to gaseous electronics (see Thomson and Rutherford, 1896), has been reviewed by Mahan (1973), and has seen a recent revival of interest because of its role in the kinetics of rare-gas/halogen laser media (see for example, Flannery and Yang, 1978; and Wadehra and Bardsley, 1978).

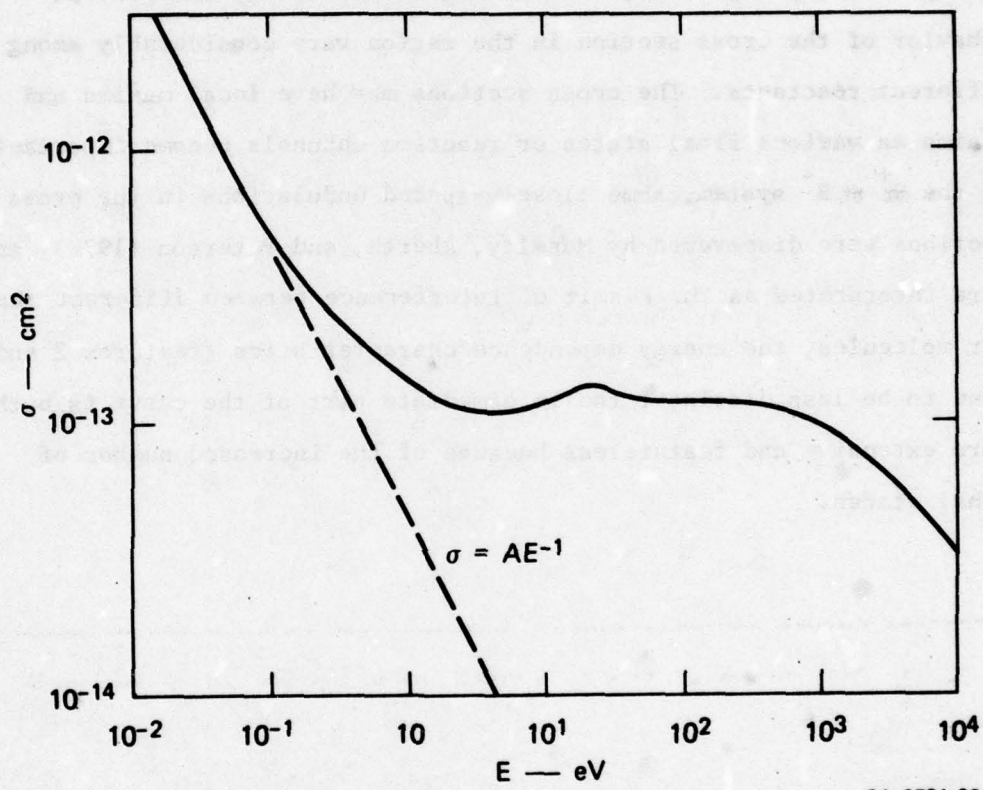
Mutual neutralization reactions are important in ionized gases because of their large cross sections, attributable to the coulomb interaction. Binary mutual neutralization cross sections at an average relative energy E corresponding to 300 K are typically

10^{-12} cm^2 and scale as E^{-1} at low energies. Gas phase reaction rate coefficients for simple atmospheric ions in the temperature range $T = 200-300 \text{ K}$ thus tend to be about $10^{-7} \text{ cm}^3/\text{sec}$ and scale as $T^{-\frac{1}{2}}$ for temperatures $T \leq 1,000 \text{ K}$.

Despite the large cross sections, mutual neutralization reactions are difficult to study in the laboratory because of the difficulty in creating sufficiently high densities of identified and selected species of ions. Among experiments on ternary mutual neutralization, identification of the ion species involved is in question. Binary mutual neutralization experiments are in better shape, but even so, almost no work has been done on identifying the neutral products and excited states resulting from the reactions.

Ion-ion mutual neutralization forms an interesting theoretical problem because it belongs to a large class of electron-transfer processes that can be described in terms of potential curve crossing dynamics; further, it represents a case in which the shapes of the potential curves are well known. However, the calculation of mutual neutralization cross sections is complicated by the large number of potential curve crossings involved in many cases, especially with molecular species where rotational or vibrational excitation may play a role in the collision.

A typical ion-ion mutual neutralization cross section curve as a function of energy appears in Figure 1. We note several features:



SA-3784-22

Figure 1. A "typical" atomic ion-ion mutual neutralization cross section as a function of relative energy

- (1) the large cross section values, which are typically $\geq 10,000 \text{ \AA}^2$ at an energy corresponding to 300 K; (2) an E^{-1} energy dependence at very low energies ($E \leq 0.1 \text{ eV}$); (3) an E^{-1} behavior at very high energies, which is really a v^{-2} velocity dependence (independent of mass), and which may be different if dissociation occurs--see Moseley, Olson, and Peterson, (1975), pp. 33-34; and (4) a relatively flat

portion of the curve, which may even increase with E at intermediate energies. The last feature is of greatest complexity theoretically, because in that energy region, the different potential curve crossings exhibit the greatest influence. The cross sections here are also really velocity dependent, thus the extent in energy and general behavior of the cross section in the region vary considerably among different reactants. The cross sections may have local maxima and minima as various final states or reaction channels become important. In the $H^+ + H^-$ system, some closely-spaced undulations in the cross sections were discovered by Moseley, Aberth, and Peterson (1970), and were interpreted as the result of interference between different channels. For molecules, the energy dependence characteristics (features 2 and 4) tend to be less distinct; the intermediate part of the curve is both more extensive and featureless because of the increased number of final states.

II EXPERIMENTAL TECHNIQUES AND RESULTS

A. Measurements in Gases

Several careful experiments on ternary ion-ion mutual neutralization were conducted in the 1930s in x-ray excited gases, following development of the technique over many years. The experiments showed that the effective two-body rate coefficient increased as the gas pressure was increased--owing to three-body effects--but saturated for gas pressure of about 1 atm, at a value of $2-3 \times 10^{-6} \text{ cm}^3/\text{sec}$. Figure 2, for measurements in air, shows results of Sayers (1938) as open circles, and of Mächler (1936) as solid dots, compared to the theoretical model of Natanson (1959). It is interesting that despite the uncertainty in the identity of the ionic species involved,

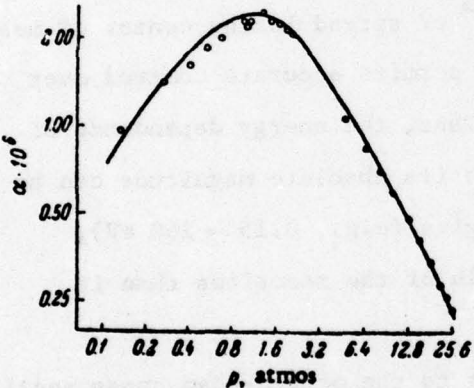


Figure 2. Typical results for three-body ion-ion mutual neutralization in air, expressed in terms of an effective binary rate coefficient. Figure from Natanson (1959).

saturation values of $2-3 \times 10^{-6} \text{ cm}^3/\text{sec}$ at 300 K are consistently reported, and that range of values may hold even for atomic ions (Wadehra and Bardsley, 1978).

More recent gas phase measurements of Mahan, and of Hirsh and Eisner, have been discussed in the reviews of Mahan (1971) and of

Moseley, Olson, and Peterson (1975), respectively. The interpretation of the data is complex.

B. Merged Beams-Technique

In the merged-beams technique, two mass-selected ion beams moving in the same direction are merged and superimposed over a known path length, and then separated by an electric field. Neutral products of reactions between the two beams pass undeflected through the field and are subsequently detected. When two fast particle beams move parallel to each other, not only can their average relative velocity be made arbitrarily small, but the velocity distributions that relate to the inherent energy spreads in the beams are dramatically reduced as the average relative velocity approaches zero, even though the laboratory energy spread is unchanged. Thus a laboratory energy spread of 1 eV in each of two parallel, merged beams of equal mass and each traveling at 2.5 keV (lab) is seen as a 5×10^{-5} eV spread in the center of mass energies. The same "deamplification" permits accurate control over the relative energies of the beams. Thus, the energy dependence of the reaction cross sections as well as its absolute magnitude can be established over a wide range of energies (e.g., 0.15 \rightarrow 200 eV), providing more insight into the details of the reactions than is possible by gas-phase methods.

In practice, the low energy limit to the merged-beam cross section measurements results from lack of complete beam collimation and alignment and was established to be about 0.15 eV. A practical limit to the collimation results from the need for sufficient ion beam currents to attain useful signal levels. The method is highly specific and can provide great detail about the reaction cross sections. It is, however, a complicated one and requires careful attention to the spatial quality of the beams and possible sources of interference.

Nevertheless, it has been highly successful for atomic and simple molecular ions, and has provided the first real opportunity to test theoretical treatments of ion-ion neutralization. The most serious problem with the technique derives from the fact that beams of molecular ions (as compared to atoms) are almost always at least vibrationally excited.

Little doubt exists as to the correctness of the merged-beams data for atomic ions. The best-studied case is that of $H^+ + H^- \rightarrow H + H$. The low energy, merged-beams data of Moseley, Aberth, and Peterson (1970) overlapped well the high-energy inclined-beam data of Rundel, Aitken, and Harrison (1969), and detailed structure can be seen in the cross section (Figure 3). The high-energy data have been improved by Gaily and Harrison (1970), and the intermediate-energy data have been improved by Peart, Grey, and Dolder (1976) who used an inclined beam method. No satisfactory, sophisticated theoretical calculation is yet available for $H^+ + H^-$. The problem is complicated by the degeneracies and the need to include rotational coupling between initial and final states when dealing with light molecules.

The collected merged beams results for atomic and molecular ions have been presented by Moseley, Olson and Peterson (1975), typically for the energy range 0.15-200 eV. Reaction rate coefficients for use in atmospheric modeling were calculated from those data, using a polynomial fit (based on the Landau-Zener theory) to extrapolate to lower energies and then averaging over a Maxwellian velocity distribution. Those rate coefficients are tabulated in Table 1. A direct comparison of the merged-beams and gas-phase results will be given below.

C. Flowing Afterglow Technique

At the University of Birmingham (UK), a gas phase technique has

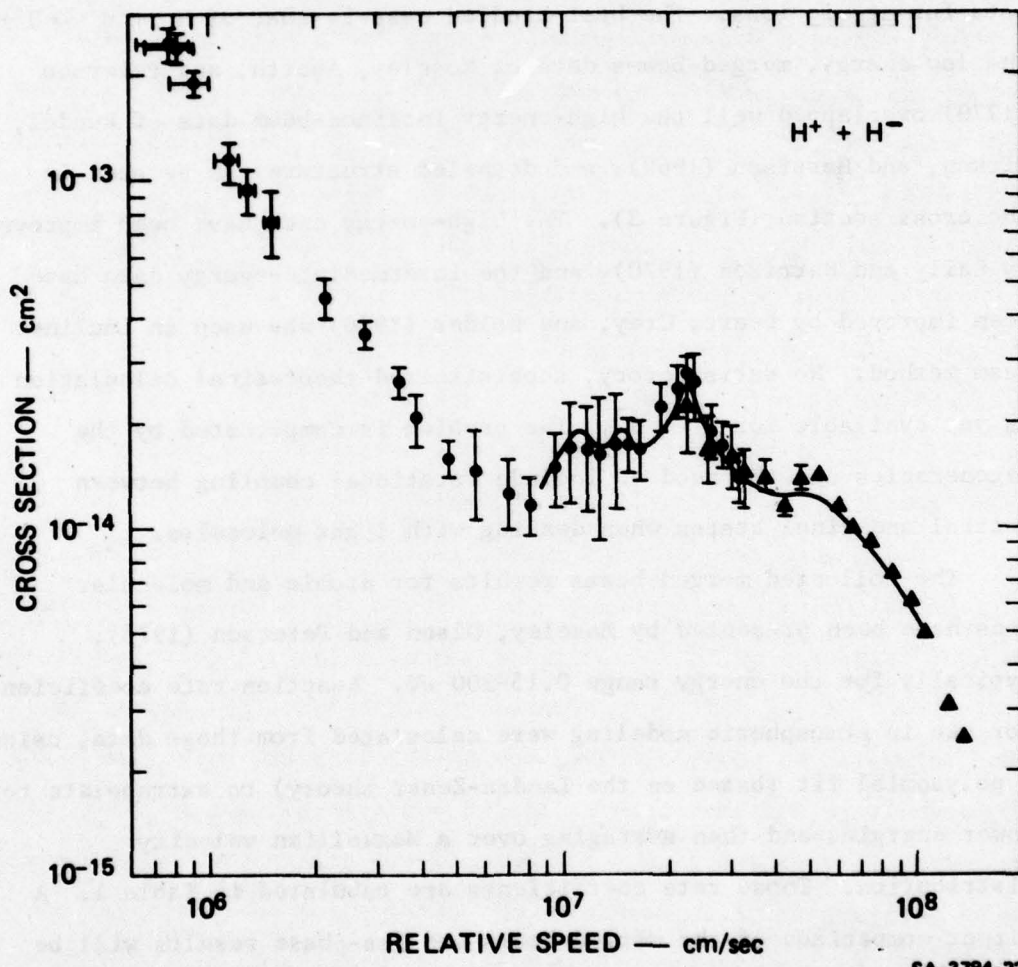


Figure 3. Experimental data for $H^+ + H^- \rightarrow H + H$ cross sections. Solid circles: Moseley, Aberth and Peterson (1970); Triangles: Rundel, Aitken and Harrison (1969), and Gaily and Harrison (1970); Continuous curve traces the data of Peart, Grey and Dolder (1976).

Table I. ION-ION MUTUAL NEUTRALIZATION RATE COEFFICIENTS AT 300 K
DEDUCED FROM MERGED BEAM MEASUREMENTS AT SRI.

Ions	$\alpha(10^{-8} \text{ cm}^3/\text{sec})$
$\text{H}^+ + \text{H}^-$	39 ± 21
$\text{N}^+ + \text{O}^-$	12 ± 3 (a)
$\text{O}^+ + \text{O}^-$	20 ± 10
$\text{Na}^+ + \text{O}^-$	21 ± 10
$\text{He}^+ + \text{H}^-$	65 ± 15 (b)
$\text{He}^+ + \text{D}^-$	52 ± 12 (b)
$\text{H}_2^+ + \text{D}^-$	47 ± 15
$\text{NO}^+ + \text{O}^-$	49 ± 20
$\text{O}_2^+ + \text{O}^-$	10 ± 4
$\text{N}_2^+ + \text{O}^-$	20 ± 10
$\text{N}_2^+ + \text{O}_2^-$	16 ± 5
$\text{NO}^+ + \text{O}_2^-$	58 ± 10
$\text{O}_2^+ + \text{O}_2^-$	42 ± 13
$\text{N}_2^+ + \text{NO}_2^-$	13 ± 5
$\text{NO}^+ + \text{NO}_2^-$	51 ± 15
$\text{NO}^+ + \text{OH}^- \cdot \text{H}_2\text{O}$	10 ± 5 (a)
$\text{O}_2^+ + \text{NO}_2^-$	41 ± 13
$\text{NO}^+ + \text{NO}_3^-$	81 ± 23
$\text{O}_2^+ + \text{NO}_3^-$	13 ± 4

^a Revised or unpublished data from Bennett et al (1974)

^b The data for $\text{He}^+ + \text{D}^-$ are limited to energies ≥ 60 eV and do not permit direct extrapolation to thermal energies. However, the data agree well with theoretical calculations that yield a 300 K rate coefficient of $52 \times 10^{-8} \text{ cm}^3/\text{sec}$ for $\text{He}^+ + \text{D}^-$ and $65 \times 10^{-8} \text{ cm}^3/\text{sec}$ for $\text{He}^+ + \text{H}^-$.

been developed for measuring ion-ion mutual neutralization rate coefficients. The Birmingham method is well-suited for atmospheric related studies because ion-ion reaction rate coefficients are measured directly, and at atmospheric temperatures (measurements have been made for 180-530 K). It should also be possible to measure three-body reaction rate coefficients.

The Birmingham group uses a flowing afterglow apparatus, with a movable Langmuir probe to determine ion densities, and a mass spectrometer downstream to identify the ion species. The afterglow tube is pyrex, 7.6 cm in diameter, about 84 cm long. The flowing buffer gas is usually helium at about 0.5 torr. Small concentrations of reactant gases may be added either upstream or downstream of a microwave discharge cavity to create desired ionic species. Positive ions are created either in the microwave discharge or by Penning ionization in the afterglow. Negative ions are created by electron attachment. The primary ions may be (and often are) converted to different species through ion-molecule reactions taking place in the flow tube. If the ion densities are great enough, ion-ion mutual neutralization dominates over ambipolar diffusion in the loss of ionization. Initial ion densities in the ion-ion plasma must be typically $3 \times 10^{10} \text{ cm}^{-3}$ to avoid diffusion effects. Using the Langmuir probe to determine both the positive and negative ion densities as a function of distance from the ion production region, the ion-ion mutual neutralization rate coefficient may be determined. The distance scale in the flow tube is converted to a time scale through a direct measurement of the plasma flow velocity, using the Langmuir probe to follow a pulsed disturbance down the length of the flow tube.

Care must be taken in the determination of the ion identities because the interpretation of the Langmuir probe current-voltage characteristics requires knowledge of the ion masses, which may be

changing along the flow tube due to ion-molecule reactions (Smith and Church, 1976). In some cases, the concentrations of the minority gases (which form the ions in a neutral buffer gas) may be adjusted so that a single negative ion and a single positive ion completely dominate the mass spectrum. In other cases, when one is attempting to study reactions between clustered ions, a mixture of ion types is likely to result and some estimate of the effective mass made. Since the ion-ion mutual neutralization rate coefficient may be determined from the decay of either the positive or negative ion densities, the investigator has some built-in duplication that aids in understanding the ion chemistry in complex cases.

Aside from the care needed in assessing the ion chemistry in the flow tube, the flowing afterglow method appears to be limited to the study of negative ions that have a fast attachment rate coefficient. If the electron attachment rate in the flow tube is not large, an ion-ion plasma cannot be produced in sufficient density that mutual neutralization dominates over diffusion. Often, species that have a large attachment rate also have a high electron affinity (EA) that tends to lower the mutual neutralization rate (Olson, 1972) though at least one known exception, SF₆ (which has a low EA but a high attachment rate), has been studied in the flowing afterglow (Church and Smith, 1977).

However, the success of the Birmingham measurements outweighs those limitations. Reaction rate coefficients have been determined for a large number of ion species, both for "simple" and clustered ions, at temperatures relevant to atmospheric studies. In Table 2 we list the data that the Birmingham group has produced. Where more than one ion species were present, an average ion-ion mutual neutralization rate coefficient was determined.

Generally, the 300 K rate coefficients determined with the flowing

Table II. ION-ION MUTUAL NEUTRALIZATION RATE COEFFICIENTS α MEASURED AT 300 K USING THE BIRMINGHAM FLOWING AFTERGLOW APPARATUS.

Ions	$\alpha(10^{-8} \text{ cm}^3/\text{sec})$
$\text{NH}_4^+ + \text{Cl}^-$	6.7 ± 0.7 (a)
$\text{NO}^+ + \text{NO}_2^-$	6.4 ± 0.7 (b)
$\text{NO}^+ + \text{NO}_3^-$	5.7 ± 0.6
$\text{NO}^+(0.7)$ } + NO_2^-	6.3 ± 0.7
$\text{NH}_4^+(0.3)$ } + NO_2^-	
$\text{CCl}_3^+(0.8)$ } + Cl^-	4.5 ± 0.5
$\text{CCl}_2^+(0.2)$ } + Cl^-	
$\text{CClF}_2^+(0.9)$ } + Cl^-	4.1 ± 0.4
$\text{CCl}_2^{\text{F}}(0.1)$ } + Cl^-	
$\text{SF}_3^+ + \text{SF}_5^-$	4.0 ± 0.5
$\text{SF}_5^+ + \text{SF}_6^-$	3.9 ± 0.5
$\text{Xe}^+ + \text{F}^-$	< 0.5
$\text{Xe}^+ + \text{Cl}^-$	≤ 0.5
$\text{Kr}^+ + \text{F}^-$	≤ 0.5
$\text{Ar}_2^+ + \text{F}^-$	≤ 0.2
$\text{Cl}_2^+ + \text{Cl}^-$	5.0
$\text{O}_2^+ + \text{CO}_3^-$	9.5
$\text{NH}_4^+ \cdot (\text{NH}_3)_2 + \text{Cl}^-$	7.9 ± 1.0
$\text{NH}_4^+ \cdot (\text{NH}_3)_2 + \text{NO}_2^-$	4.9 ± 0.6
$\text{NH}_4^+ \cdot (\text{NH}_3)_2 (0.67)$ } + NO_2^-	5.5 ± 0.6
$\text{NH}_4^+ \cdot (\text{NH}_3)_3 (0.33)$ } + NO_2^-	
$\text{NH}_4^+(0.31)$ } + $\text{NO}_2^-(0.47)$	
$\text{NH}_4^+(0.25)$ } + $\text{NO}_3^-(0.53)$	9.6 ± 1.3
$\text{NH}_4^+ \cdot \text{NH}_3(0.25)$ } + $\text{NO}_3^-(0.53)$	
$\text{NH}_4^+ \cdot (\text{NH}_3)_2 (0.19)$	

Table II Continued

Ions	$\alpha (10^{-8} \text{ cm}^3/\text{sec})$
$\left. \begin{array}{l} \text{NH}_4^+ (0.16) \\ \text{NO}^+ (0.16) \\ \text{NO}_2^+ (0.19) \\ \text{NH}_4^+ \cdot \text{NH}_3^- (0.23) \\ \text{NH}_4^+ \cdot (\text{NH}_3^-)_2 (0.26) \end{array} \right\} + \left. \begin{array}{l} \text{NO}_3^- (0.19) \\ \text{NO}_3^- \cdot \text{HNO}_3^- (0.38) \\ \text{NO}_3^- \cdot (\text{HNO}_3^-)_2 (0.43) \end{array} \right\}$	5.8 ± 0.9
$\left. \begin{array}{l} \text{NH}_4^+ \cdot \text{NH}_3^- (0.27) \\ \text{NH}_4^+ \cdot (\text{NH}_3^-)_2 (0.33) \\ \text{NH}_4^+ \cdot (\text{NH}_3^-)_3 (0.40) \end{array} \right\} + \left. \begin{array}{l} \text{NO}_3^- (0.30) \\ \text{NO}_3^- \cdot \text{HNO}_3^- (0.33) \\ \text{NO}_3^- \cdot (\text{HNO}_3^-)_2 (0.37) \end{array} \right\}$	6.1 ± 1.0
$\text{H}_3\text{O}^+ \cdot (\text{H}_2\text{O})_3 + \text{Cl}^-$	4.8 ± 0.6
$\text{H}_3\text{O}^+ \cdot (\text{H}_2\text{O})_3 + \text{NO}_3^-$ (and minority species)	5.5 ± 1.0
$\text{H}_3\text{O}^+ \cdot (\text{H}_2\text{O})_3 + \text{NO}_3^- \cdot \text{HNO}_3^-$ (and minority species)	5.7 ± 1.0
$\text{NO}^- \cdot (\text{NO}_2^-)_2 + \text{NO}_3^- \cdot (\text{HNO}_3^-)_3$	3.5 (c)

Note: When more than one positive or negative ion species was present, the fractional concentrations are given in parentheses.

^a Measurements at other temperatures: $\alpha = 8.3 \pm 1.0$ at 220 K, and $\alpha = 5.6 \pm 1.3$ at 430 K, in units of $10^{-8} \text{ cm}^3/\text{sec}$.

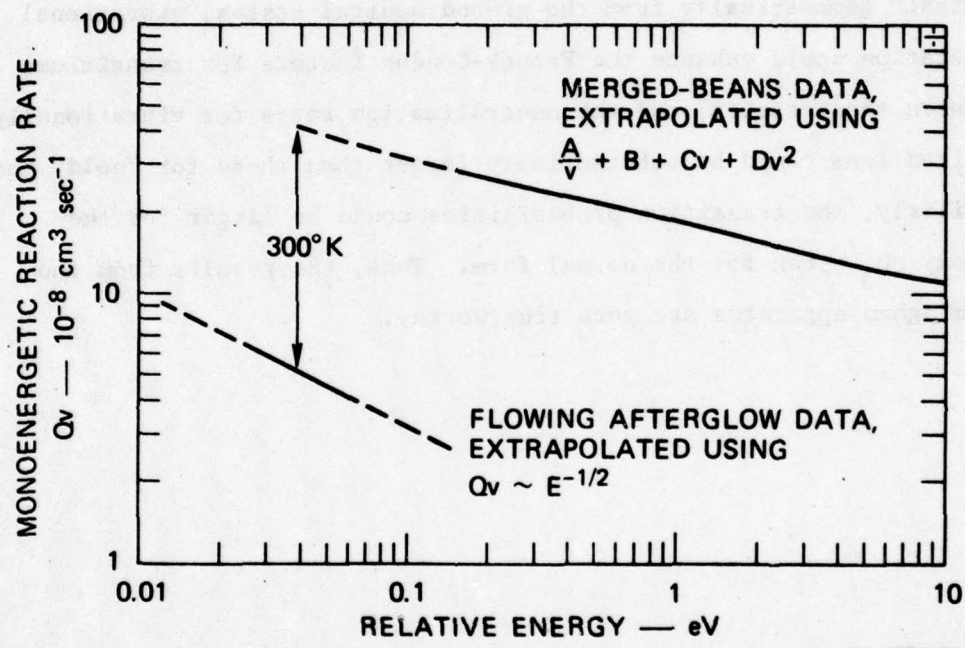
^b Measurements at other temperatures: $\alpha = 8.4 \pm 1.0$ at 185 K, 6.4 ± 0.8 at 420 K, and 5.8 ± 0.6 at 530 K, in units of $10^{-8} \text{ cm}^3/\text{sec}$.

^c Reaction studied at 182 K. If $\alpha \sim T^{-\frac{1}{2}}$, then $\alpha = 4.5 \times 10^{-8} \text{ cm}^3/\text{sec}$ at 182 K can be used to derive a rate coefficient at 300 K as given above.

afterglow apparatus are lower than those deduced from the merged-beams data, although there is little direct overlap (two cases) between the ion species studied. Both sets of results tend to be within a factor of 2 of the absorbing-sphere theoretical values, with the flowing afterglow results lower and the merged beams results higher. Mutual neutralization rate coefficients for atomic ions show a large variation, which is understandable in terms of the varied locations of potential curve crossings, the number of crossings, and the ion masses. The flowing afterglow data for molecular ions seem to imply that the presence of many electronic states and of internal degrees of freedom tends to narrow the range of values of the rate coefficients, although the effects of mass and electron affinity are certainly present. The data obtained on the Birmingham apparatus thus far yield rate coefficients in the range $4-10 \times 10^{-8} \text{ cm}^3/\text{sec}$ and indicate that a value of $6 \times 10^{-8} \text{ cm}^3/\text{sec}$ at 300 K is a good estimate of the mutual neutralization rate coefficient for the complex molecular ions if one wishes to choose a single value, without regard to the precise species involved.

We have stated earlier that the flowing afterglow rate coefficients (300 K) tend to be smaller than those deduced from the merged-beams data. Only two reactions have been studied in common between those apparatuses, $\text{NO}^+ + \text{NO}_2^-$ and $\text{NO}^+ + \text{NO}_3^-$. Unfortunately, the merged-beams results for those two reactions were much larger than the body of results for all other reactions studied with that apparatus, and the belief is that those beam ions were partially excited. However, it is still interesting to see a comparison between the flowing afterglow data and the merged-beams data for a particular case, $\text{NO}^+ + \text{NO}_2^-$. For this comparison, the flowing afterglow thermal rate coefficients were converted to monoenergetic rates (cross section

times relative velocity) and the results are shown in Figure 4. Two points are made: the merged-beams results are almost 10 times greater than the flowing afterglow results (and the two cannot be reconciled by a different extrapolation procedure), and the energy dependence of the flowing afterglow data agrees with theoretical expectations at low energies, $Qv \sim E^{-1/2}$, whereas the merged-beams data show a slower decrease with energy.



SA-3784-24

Figure 4 A comparison of merged-beams data and flowing afterglow data for the ion-ion mutual neutralization reaction
 $\text{NO}^+ + \text{NO}_2^- \rightarrow \text{neutral products}$

As a test for excitation in the merged-beam ions, one series of experiments was made to determine if the NO^+ ions were in the metastable $a^3\Sigma^+$ state. Charge transfer attenuation of NO^+ beams passing through Ar gas were made in the manner of Turner, Rutherford,

and Compton (1968), and it was concluded that less than 10% of the ions were excited. Similar tests were made to see if NO_2^- ions formed in different gases were vibrationally excited, but the tests were inconclusive. Very likely, both the NO_2^- and NO_3^- ions were at least vibrationally excited, and the possibility also exists that some of the NO_3^- ions were in the isomeric "peroxy" state. Because the ground electronic states of the negative ions are generally "offset" geometrically from the ground neutral states, vibrational excitation could enhance the Franck-Condon factors for transitions between these states, and the neutralization rates for vibrationally excited ions could be substantially larger than those for "cold" ions. Similarly, the transition probabilities could be larger for the peroxy NO_3^- than for the normal form. Thus, the results from the Birmingham apparatus are more trustworthy.

III THEORY

The basic ideas in the theoretical description of ion-ion mutual neutralization have been reviewed by Moseley et al. (1975). With the assumption that electron transfer takes place at avoided crossings of the ionic and covalent potential curves for the interacting systems, the Landau-Zener theory may be used to calculate the mutual neutralization cross section provided that (a) the coupling matrix element can be calculated for each crossing, (b) the excited states of the neutral system are known in order to determine the asymptotic covalent potential curves, and (c) not too many states are involved so that the problem may be tractable. An appropriate formula for the matrix elements connecting the initial and final states has been deduced by Olson, Smith, and Bauer (1971) by correlating a large number of ab initio calculations and experimental data on electron transfer. In regard to the number of covalent states involved, there are two extremes:

- (a) If only one or two covalent states are possible as product channels, a close-coupling calculation may be carried out instead of using the Landau-Zener theory. The close-coupling calculation takes account of interactions over an extended region of internuclear separations near an avoided crossing rather than just at the point of closest approach between two interacting states. Olson (1977) has carried out close-coupling calculations for $\text{Na}^+ + \text{Cl}^-$ and $\text{K}^+ + \text{Cl}^-$, where there is nominally only one avoided crossing, but spin-orbit splitting induces a second crossing. For KCl, it is noteworthy that Olson found Landau-Zener cross sections to be several orders of magnitude too small (compared with the more reliable close-coupling results) because the avoided crossings take place at large internuclear distance ($\sim 20 \text{ \AA}$) where the Landau-Zener description of the interaction is inadequate.

(b) If there is a large number (≥ 10) of covalent states crossing the ionic potential, as is common for molecular systems, Olson (1972) has developed an "absorbing sphere" model that avoids calculating transition probabilities for each curve crossing. The model seems to be quite successful, and the results are dependent only on the electron detachment energy of the negative ion and the reduced mass of the system (Moseley et al., 1975).

Emphasis in recent years has been on mutual neutralization of large ionic clusters, motivated by the realization that such clusters dominate in the nighttime quiescent atmosphere at altitudes below about 85 km when negative ions are most important. With molecular ions, one interesting problem is to determine how excitation of internal vibrational and rotational degrees of freedom during the collisions affects the mutual neutralization cross sections. If the excitation takes place at long ranges, the cross section may be increased, because absorption of the available kinetic energy (kT) can trap the ions in orbiting states and increase the probability of electron transfer. The clustering of neutral molecules to an ion core, e.g., $\text{H}_3\text{O}^+ \cdot (\text{H}_2\text{O})_n$, will affect the mutual neutralization cross sections both through altered curve crossings (both in number and crossing distance) and by increasing the number of internal degrees of freedom. In addition, the increased mass of clustered ions will tend to lower the reaction rates because of the decrease in thermal velocities. The SRI group has considered the fact that the bonding of enough water molecules to an ion could result in the lowering of the ionic curve below all covalent ones, so that mutual neutralization could occur only by coalescence of the positive and negative ions into an ionic complex, with internal (vibrational) excitation absorbing the binding energy (Bennett et al., 1974).

A detailed calculation of absolute cross sections for the mutual neutralization of large clustered ions is extremely difficult because of the large number of electronic states and external degrees of freedom.

A more reasonable goal is to determine the dependence of the cross sections on the number of added molecules, their dipole moments, and their binding energies.

We will describe here the historical developments in our research to this problem. In an earlier report we gave estimates of neutralization rates for hydrated ions (Bennett et al., 1974). We have examined the ion-ion neutralization theory for hydrated (or other cluster) ions. This extends our earlier results, which applied to moderately large clusters (with average hydration number $\bar{n} \geq 6$), to smaller clusters ($1 \leq \bar{n} \leq 6$).

Olson's absorbing sphere version of the curve-crossing theory of neutralization is highly effective for many small molecular ions, but it is probably inapplicable for the hydrated (cluster) ions. The absorbing sphere model does not consider that the initial ion and product neutral minimum energy states probably have substantially different configurations and internuclear separations, with correspondingly small Franck-Condon factors between the initial and final states of the electron capture transitions. Such an effect would reduce the transition probabilities. Likewise, the model does not account for the "tidal" orbital trapping that can result from the excitation of internal vibrational and rotational modes during the collision. That effect will increase the transition probabilities. To consider these effects, we first took a radically different approach to obtain upper and lower limits to neutralization rates, independent of electronic transitions. Part of it follows the results of our earlier considerations (Bennett et al., 1974).

For cluster ions of any size, close encounters within a distance r_c of typical molecular dimensions will lead to a hard impact, with almost certain internal excitation or fragmentation, permanent trapping, and inevitable neutralization. The term r_c depends on \bar{n} but not on the relative energy E_r . The cross section depends on E_r and \bar{n} as

$$\sigma \approx \frac{\pi e^2 r_c(\bar{n})}{E_r} \quad . \quad (3)$$

This hard-impact mechanism leads to a lower-bound rate coefficient for hydrated ions of magnitude

$$k_l = k_c \approx 7 \times 10^{-8} \frac{\text{cm}^3}{\text{sec}} \left(\frac{300 \text{ K}}{T} \right)^{\frac{1}{2}} (\bar{n})^{-1/6} \quad . \quad (4)$$

for any $\bar{n} \geq 1$.

Collisions outside the close-encounter range r_c but inside some larger tidal trapping range r_t may also lead to neutralization, but not necessarily. The tidal trapping range r_t depends on E_r as well as on \bar{n} , and the trapping probability may be much less than unity, especially for small \bar{n} ($1 \leq \bar{n} \leq 5$); the trapping cross section σ_t is then less than some upper bound σ_u ,

$$\sigma_t \leq \sigma_u \approx \frac{\pi e^2 r_t (E_r, \bar{n})}{E_r} \quad . \quad (5)$$

After trapping, neutralization follows with almost unit probability if there are enough internal degrees of freedom, i.e., if \bar{n} is moderate to large (≥ 3); it may be less probable, however, for \bar{n} near unity.

If we write $k_{n,t}$ for the rate coefficient for neutralization by the tidal trapping mechanism, the total neutralization rate coefficient is the sum:

$$k_n(T, \bar{n}) = k_c(T, \bar{n}) + k_{n,t}(T, \bar{n}) \quad . \quad (6)$$

The total k_n is less than an upper bound k_u related to σ_u , $k_n(T, \bar{n}) \leq k_u(T, \bar{n})$. On the basis of a simple electrostatic model, we previously estimated k_u to be

$$k_u(T, \bar{n}) \approx 1.2 \times 10^{-6} \left(\frac{300 \text{ K}}{T} \right) (\bar{n})^{-\frac{1}{2}} \quad . \quad (7)$$

While $k_l(T, \bar{n})$ is expected to be a good approximation to the close-coupling encounter rate k_c , the difference $(k_u - k_l)$ is not necessarily a

good estimate of the tidal neutralization rate $k_{n,t}$, and may be much larger. That is because k_u is an estimate based on a static distortion model that neglects dynamic effects. Especially when the number of internal degrees of freedom is small, as when $\bar{n} = 1$ or 2, these dynamic effects may severely limit the probability of tidal trapping or of subsequent neutralization. Consequently, we expect $k_{n,t}$ to be small when \bar{n} is small (perhaps even smaller than k_c), and then to rise gradually with increasing \bar{n} to some limit approaching $(k_u - k_c)$. Correspondingly, the total neutralization rate will rise from near k_u at low \bar{n} to near k_u at large \bar{n} .

This general picture seems to be in reasonable agreement with the experimental information, especially the data on small cluster ions from the Birmingham group, which generally show room-temperature rates near $6 \times 10^{-8} \text{ cm}^3/\text{sec}$ (Smith, Church, and Miller, 1978).

A. P. Hickman (1978) contributed the next step in the theoretical treatment, developing a model for the quantitative calculation of the $\text{O}^- + \text{NO}^+$ and $\text{O}^- + \text{NO}^+ \cdot \text{H}_2\text{O}$ reaction rates. The model considers separately both the electron transfer and internal excitation processes. Only the lowest frequency rotational and vibrational modes were considered, but the effective increase in the ionization energy of the clustered NO^+ ion was included. The effects of orbiting on the electron transfer probabilities were not examined, but otherwise, the effects of internal excitation were found to be minimal in such simple clusters; the dominant effects of clustering were caused by changes in the mass and in the electron affinity. An approximate scaling formula was obtained that fits a wide range of experimental data involving simple ions and small clusters. This scaling rule relates the rate constant for recombination (α) to the electron affinity of the electron donor (EA) and the reduced collision mass (m):

$$\alpha^{-1} = C(T/300 \text{ K})^{0.5} m^{0.5} (\text{EA})^{0.4}$$

If the units of α , m , and EA are cm^3/sec , atomic units and eV, respectively, then $C = 4.38 \times 10^4$. This formula fits a wide variety of experimental data with an accuracy of about $\pm 30\%$, as shown in Figure 5. A preprint of a paper describing this work is included as an Appendix.

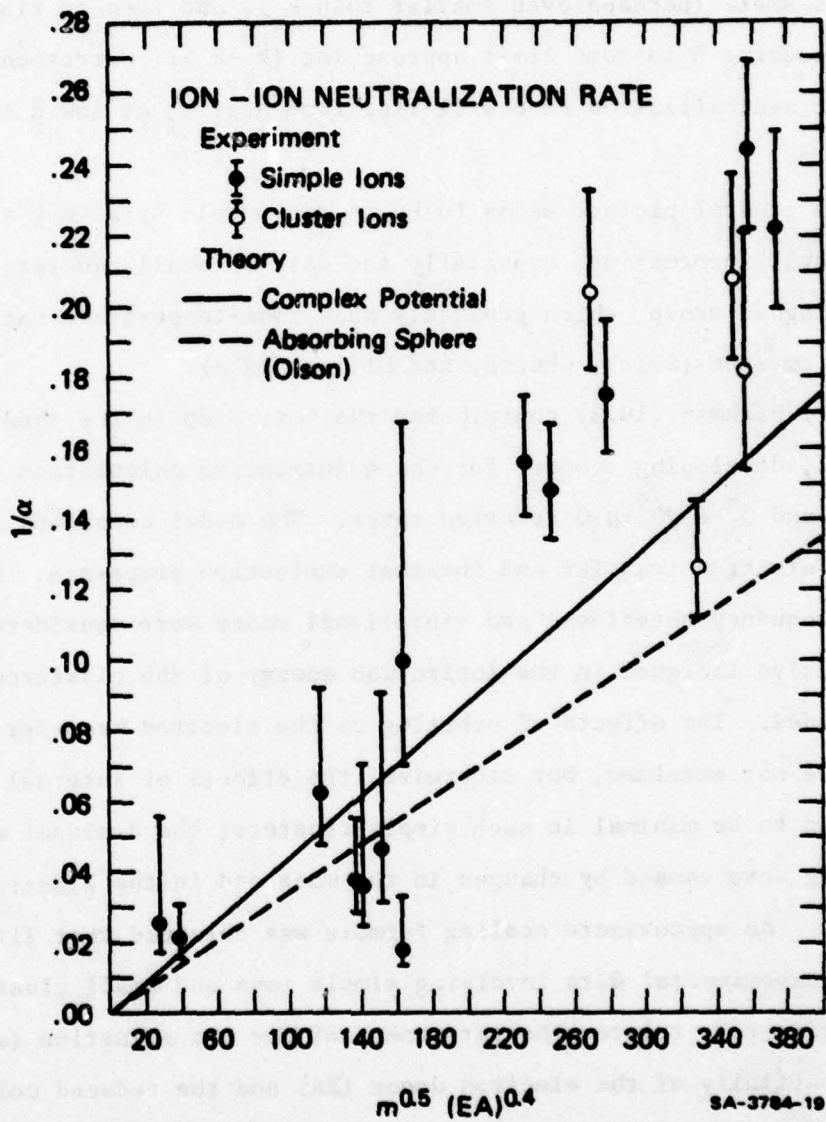


Figure 5. Comparison between recent theoretical results and experimental data from several laboratories. The complex potential approach does not invoke adjustable parameters. Units are as follows: $\alpha: 10^8 \text{ cm}^3/\text{sec}$; m : atomic units; EA: electron volts.

IV ATMOSPHERIC IMPLICATIONS

The process of mutual neutralization of ions in the atmosphere is a complicated function of altitude. Three altitude-dependent variables must be considered: (1) the type of positive and negative ions present; (2) the temperature; and (3) the neutral gas density. In the stratosphere, below about 30 km altitude, the ions are all in the form of large clusters. Since the stratosphere contains few free electrons, mutual neutralization is the dominant process for the removal of ions. Furthermore, the gas density is high enough that three-body neutralization is effective. At higher altitudes, the ion species become somewhat simpler, and the gas density is such that binary mutual neutralization dominates. A good summary of average mutual neutralization rate coefficients in the atmosphere appears in a chart by Smith and Church (1977), which is reproduced as Figure 6. The figure shows likely positive and negative ion types and the appropriate ionic recombination coefficients deduced from flowing afterglow and other experiments.

n (cm^{-3})	h (km)	Temperature (K)	Positive ions	Est. mass (amu)	Negative ions	Est. mass (amu)	μ (amu)	Binary α ($\text{cm}^3 \text{s}^{-1}$)	Ternary α_3 ($\text{cm}^3 \text{s}^{-1}$)	Total α_t ($\text{cm}^3 \text{s}^{-1}$)	Comments	References to observed and calculated ion types
7(13)	90	Mesopause	NO^+ O_2^+	0*	O_2^-							Arnold et al., 1974
4(14)	~80		$\text{H}_3\text{O}^+ \cdot (\text{H}_2\text{O})_n$ $n = 3$	(30)	CO_3^- Cl^- HCO_3^-	(50)	25	9.0(-8)		9.0(-8)	NO^+ changeover to water clusters (nighttime)	Arnold et al., 1971
2(15)	~70				NO_3^-							Narcisi et al., 1971, 1972
6(15)	~60		$\text{H}_3\text{O}^+ \cdot (\text{H}_2\text{O})_n$ $n = 3, 4$	(80)	$\text{NO}_3^- \cdot (\text{H}_2\text{O})_q$ $q = 1-5$	(100)	45	6.5(-8)		6.5(-8)	Transition from electron-ion to ion-ion recombination	Thomas, 1974
2(16)	~50	Stratopause							2(-9)	8(-8)		Spielvogel and Thorne, 1975
8(16)	~40		$\text{H}_3\text{O}^+ \cdot (\text{H}_2\text{O})_n$ $n = 4, 5, 6$	(110)	$\text{NO}_3^- \cdot (\text{H}_2\text{O})_q$ $q = 5$ (estimated)	(150)	65	5.0(-8)	2.5(-8)	7.5(-8)		Mohnen, 1971
4(17)	~30								1.5(-7)	2(-7)	Binary recombination	Fensentoefeld et al., 1975
2(18)	~20		$\text{H}_3\text{O}^+ \cdot (\text{H}_2\text{O})_n$ $n = 6$	(130)	$\text{NO}_3^- \cdot (\text{H}_2\text{O})_q$ $q > 5$	(170)	75	5.0(-8)		7.5(-7)	Ternary recombination	Fensentoefeld and Ferguson, 1975
8(18)	~10	Tropo- pause	$\text{NH}_4^+ \cdot (\text{NH}_3)_m \cdot (\text{H}_2\text{O})_p$ $m + p = 6$		$\text{NO}_3^- \cdot (\text{HNO}_3)_r$ $r = 2$				3.5(-6)	3.5(-6)	Saturated ternary recombination	Fensentoefeld et al., 1975
4(19)	0-150								3(-8)	3(-8)		

Figure 6. The earth's atmosphere: sea-level to 90 km. [Smith and Church (1977)]

The average rate coefficients are not based on measurements for all known atmospheric ion species, convoluted with an atmospheric model. Rather, they are based on the fact that the binary rate coefficients measured with the Birmingham flowing afterglow apparatus do not vary much with ion identity at a fixed temperature, and that the temperature dependence of the measured rate coefficients seems to fit the $T^{-\frac{1}{2}}$ dependence predicted by theory. The three-body estimates are perhaps cruder. Smith et al. (1978) conclude that the temperature dependence of the average mutual neutralization rate coefficient is probably a more important consideration in atmospheric modeling than is precise knowledge of the ion species.

In the disturbed atmosphere, the ionospheric layers are lowered in altitude. Depending on the type of disturbance (solar proton shower, nuclear blast, etc.) there may be a temperature change associated with the altitude adjustment, and there will also be a trend toward simpler ion species at a given altitude, as the ionization source strength increases. If the amount of ionization versus altitude can be specified for a certain disturbance, then Figure 6 can be adjusted to give approximate mutual neutralization rate coefficients for the disturbed atmosphere. The only radical change that might be expected would be at high altitudes (> 70 km), where a significant concentration of atomic and unclustered molecular ions could lead to a wide range of mutual neutralization rate coefficients, depending on the ion types present. In general, the simpler atmospheric ions should lead to higher neutralization rates (e.g.: $3 \times 10^{-7} \text{ cm}^3/\text{sec}$ for $\text{N}^+ + \text{O}^-$ and $\text{O}^+ + \text{O}^-$).

V FUTURE WORK

A great deal has been accomplished thus far in understanding ion-ion mutual neutralization. The basic electron transfer mechanism is clear. For atomic ions, good calculations have been shown to be feasible when the computation time is warranted (Olson, 1977). Approximate theory has been worked out for molecular ions (Olson, 1972), and the first steps have been taken to treat cluster ions quantitatively (Hickman, 1978). Theoretical research is in progress at SRI to determine how those ideas must be modified for larger ions, the clusters that occur in the atmosphere. Experimentally, merged-beams and inclined-beams apparatus have been used to measure mutual neutralization reaction cross sections over a wide energy range, and basic curve-crossing theoretical models can account for the general characteristics. Flowing-afterglow experiments have provided reaction rate coefficients for simple and clustered atmospheric molecular ions, at atmospheric temperatures.

The thrust of future work should be to reach a better understanding of the neutralization of clustered ions in the atmosphere. Theoretical research can be expected to determine cross-section dependencies on molecular properties such as the degree of clustering, bond strengths, and dipole moments. Many more results from flowing-afterglow experiments on ion cluster neutralization will be necessary to verify the trends predicted by theory. Furthermore, such data would test the preliminary indication from flow tube results that the neutralization rate coefficients do not vary much (a factor of 2) between different clusters. The flowing afterglow method can also be used to study three-body mutual neutralization, and presumably such work will be done.

Technology exists today that, in principle, would allow merged-beams experiments to be carried out with clustered ions, using high-pressure,

nozzle-expansion beam sources and cryogenic vacuum pumping. However, such experiments are very difficult and the rewards do not currently seem worth the effort and expense, in view of declining budgets.

Finally, we should point out that knowledge of the cross section is a solution to only half of the ion-ion mutual neutralization problem. Very little is known about the final states of the neutral products (see Moseley et al., 1975). However, workers at the University of Birmingham have recently used a monochromator with their flowing afterglow apparatus to observe radiation resulting from ion-ion mutual neutralization reactions.

REFERENCES

R. A. Bennett, D. L. Huestis, J. T. Moseley, D. Mukherjee, R. E. Olson, S. W. Benson, J. R. Peterson, and F. T. Smith, Investigation of Ion-Ion Recombination Cross Sections, Final Report on SRI Project PYU-1640, Air Force Cambridge Research Laboratory, Report AFCRL-TR-74-0417 (1974).

M. J. Church and D. Smith, Int. J. Mass. Spectr. Ion Phys. 23, 137 (1977).

M. R. Flannery and T. P. Yang, Appl. Phys. Lett. 32, 327, 356 (1978); 33, 574 (1978).

T. D. Gaily and M.F.A. Harrison, J. Phys. B 3, L25 (1970).

A. P. Hickman, "Approximate Scaling Formula for Ion-Ion Mutual Neutralization Rates," to be published in J. Chem. Phys. (1979).

W. Mächler, Z. Physik 104, 1 (1936).

B. A. Mahan, Adv. Chem. Phys. 23, 1 (1973).

J. T. Moseley, R. E. Olson, and J. R. Peterson, Case Studies in Atomic Physics 5, 1 (1975).

J. T. Moseley, W. Aberth, and J. R. Peterson, Phys. Rev. Lett. 24, 435 (1970).

G. L. Natanson, Soviet Phys.-Tech. Phys. 4, 1263 (1959).

R. E. Olson, Combustion and Flame 30, 243 (1977); J. Chem. Phys. 56, 2979 (1972).

R. E. Olson, F. T. Smith, and E. Bauer, Appl. Opt. 10, 1848 (1971).

B. Peart, R. Grey, and K. Dolder, J. Phys. B 9, L369 (1976).

R. D. Rundel, R. L. Aitken, and M.F.A. Harrison, J. Phys. B 2, 954 (1969).

J. Sayers, Proc. Roy. Soc. (London) A-169, 83 (1938).

D. Smith and M. J. Church, Inst. J. Mass. Spectr. Ion Phys. 19, 185 (1976); Planet. Space Sci. 25, 433 (1977).

D. Smith, M. J. Church, and T. M. Miller, J. Chem. Phys. 68, 1224 (1978).

J. J. Thomson and E. Rutherford, Phil. Mag. 42, 392 (1896).

B. R. Turner, J. A. Rutherford, and D.M.J. Compton, J. Chem. Phys. 48, 1602 (1968).

J. M. Wadehra and J. N. Bardsley, Appl. Phys. Lett. 32, 76 (1978).

APPENDICES

T. M. Miller of SRI spent the period 16 May-30 September 1977 working on ion-ion mutual neutralization experiments at the University of Birmingham, using a flowing-afterglow apparatus with Langmuir probe diagnostics. A paper was published recently in the Journal of Chemical Physics on the flowing-afterglow experiments at Birmingham during that period of collaboration, and its abstract is attached here as Appendix A.

In the University of Birmingham Ionic Physics Laboratory, the flowing afterglow apparatus shares some crucial equipment with a Selected Ion Flow Tube (SIFT) apparatus. During Dr. Miller's stay in Birmingham, he took part in SIFT experiments in which ion-molecule reactions were studied in regard to the stratosphere. The abstract of the paper describing that work appears here as Appendix B.

Appendices C through F are abstracts of the theoretical papers already published under this contract, and Appendix G is a preprint of a theoretical paper to be published in 1979 in the Journal of Chemical Physics.

Appendix A

J. Chem. Phys. 68, 1224 (1978)

Mutual neutralization of simple and clustered positive and negative ions^{a)}

David Smith, Michael J. Church, and Thomas M. Miller^{b)}

Department of Space Research, University of Birmingham, Birmingham B15 2TT, England
(Received 14 September 1977)

Measurements are reported of the rate coefficients, α , for several ion-ion mutual neutralization reactions principally involving NH_4^+ ions and their ammonia clusters $\text{NH}_4^+ \cdot (\text{NH}_3)_{1,2,3}$ with several different negative ions. The data were obtained utilizing an ion-ion flowing afterglow plasma combined with Langmuir probe diagnostics. Most of the measurements were obtained at 300 K although the $\text{NH}_4^+ + \text{Cl}^-$ reaction has also been studied at 220 and 430 K. Both the absolute magnitude of α and its temperature variation are shown to be in acceptable agreement with theoretical predictions. The α for the cluster ion reactions are very similar to those for the simpler ions, even when both positive and negative ions are large clusters, although an increase in the mean reaction cross section for the cluster ion reactions is discernible. All the α measured to date for both simple and cluster ion reactions, albeit for species of high electron affinity and over the limited temperature range of 180 to 530 K, are within the range $(4-10) \times 10^{-8} \text{ cm}^3 \text{ s}^{-1}$, more marked variations occurring with temperature than with ionic mass.

Appendix B

J. Chem. Phys. 69, 308 (1978)

A laboratory study of the reactions of N^+ , N_2^+ , N_3^+ , N_4^+ , O^+ , O_2^+ , and NO^+ ions with several molecules at 300 K

D. Smith, N. G. Adams, and T. M. Miller^{a)} b)

Department of Space Research, University of Birmingham, Birmingham B15 2TT, England
(Received 17 January 1978)

A study has been made of the rate coefficients and product ion distributions for the reactions at 300 K of the ions N^+ , N_2^+ , N_3^+ , N_4^+ , O^+ , O_2^+ , and NO^+ with CH_3NH_2 , NH_3 , H_2S , CH_3OH , H_2CO , COS , O_2 , H_2O , CH_4 , CO_2 , CO , H_2 , and N_2 molecules listed in increasing order of their ionization energies. These measurements are intended as a contribution to stratospheric chemistry. In the binary reactions of the ions of large recombination energy with molecules of low ionization energy, multiple ion products generally result and the rate coefficients are close to gas kinetic. Conversely, the low recombination energy ions NO^+ and O_2^+ generally undergo ternary association reactions with the large ionization energy molecules. The reactions of N_2^+ and N_3^+ are very similar, the most common mechanism apparently being direct charge transfer usually followed by fragmentation, the nitrogen-nitrogen bonds in the reacting ions remaining intact. The N^+ and N_4^+ reactions differ from the N_2^+ and N_3^+ reactions in that they show a greater propensity to form $N-X$ bonds, $X = O$, C , S , H , etc. The O^+ and O_2^+ reactions generally proceed via direct charge transfer where energetically possible.

Appendix C

Phys. Rev. Lett. 35, 1073 (1975)

Semiclassical Perturbation Scattering by a Rigid Dipole*

F. T. Smith, D. L. Huestis, and D. Mukherjee
Stanford Research Institute, Menlo Park, California 94025

and

W. H. Miller
Department of Chemistry, University of California, Berkeley, California 94720
(Received 31 July 1975)

A uniform semiclassical S matrix has been developed for collisions of charged particles with rotating rigid dipoles, with use of first-order perturbation theory. The resulting expression is analytical, depending on tabulated functions, and trivial to calculate; it allows evaluations of quantum transitions in classically forbidden regions, and of quantum interference effects.

Appendix D

Phys. Rev. A 17, 939 (1978)

Semiclassical perturbation theory of electron-molecule collisions

W. H. Miller

Department of Chemistry, University of California, Berkeley, California 94720

F. T. Smith

SRI International, Menlo Park, California 94025

(Received 25 July 1977)

The theory of the classical or semiclassical S matrix is combined with the use of perturbation dynamics to derive an approximately unitary expression for the scattering matrix for a very general class of potential interactions. The S matrix takes the form of a sum over products of Bessel functions whose orders are related to the changes in quantum numbers occurring in the transition, and whose arguments depend on the dynamical variables of the problem, including the unperturbed quantum numbers. In the general case, these arguments can be expressed as simple integrals over the unperturbed trajectory, and for well-behaved potentials they can be explicitly evaluated in terms of the modified Bessel functions K_0 and K_1 . The connection between the semiclassical perturbation scattering theory and other approximations, such as the Born and eikonal approximations, is demonstrated. The general theory is illustrated by applications to electron- (or ion-) polar-molecule scattering, including quadrupole as well as dipole interactions and including coupling to vibrations in both harmonic and anharmonic approximations. The more complicated interactions involve lengthier products of Bessel functions in the sum-and-product representation, but these are easily and systematically evaluated, and they reduce smoothly to the appropriate simpler expressions when the coupling coefficients of the higher-order terms become small. More complicated potentials, including interactions between polyatomic molecules, can be handled by a simple systematic extension of the same principles. For electron-molecule scattering, these expressions can be used in their present form since the sums are dominated by Bessel functions of comparatively low order which can be evaluated directly; extensions to molecule-molecule scattering and ion-molecule scattering are equally valid formally, but their practical application will often require the use of asymptotic approximations to the Bessel functions.

Appendix E

Phys. Rev. A 17, 954 (1978).

Semiclassical perturbation theory of electron-polar-molecule collisions: Total excitation and scattering cross sections

D. Mukherjee* and F. T. Smith

Molecular Physics Center, SRI International, Menlo Park, California 94025

(Received 25 July 1977)

Semiclassical perturbation scattering theory is applied to electron-polar-molecule scattering. Cross sections for elastic and rotationally inelastic transitions are obtained for $\Delta j = 0, 1, 2, 3, 4$, in the case of a pure charge-dipole interaction potential. Results are presented in terms of functions of dimensionless parameters involving the moment of inertia I and dipole moment μ of the target, and the mass, charge, and energy of the projectile. A range of these parameters sufficient to describe most situations of practical interest is explored. Significant oscillations are found in the cross sections for $|\Delta j| = 0$ and 2 as a function of dipole strength $\beta = m\mu e/\hbar^2$. For $|\Delta j| = 1$, the Born approximation is shown to be appropriate for $\beta \ll 1$, and invalid for $\beta \approx 1$ or > 1 . Scaling rules are deduced which should aid in the correlation and extrapolation of quantal calculations on specific systems. With the guidance of the Born approximation, scaling principles are also suggested for differential scattering.

Appendix F

Phys. Rev. A 17, 968 (1978)

Momentum transfer in electron-polar-molecule collisions: Results of semiclassical perturbation scattering theory

A. P. Hickman and F. T. Smith

Molecular Physics Center, SRI International, Menlo Park, California 94025

(Received 25 July 1977; revised manuscript received 13 February 1978)

Semiclassical perturbation scattering theory is applied to electron-polar-molecule collisions, assuming a pure charge-dipole interaction potential. Cross sections for momentum transfer are given in terms of dimensionless parameters involving the moment of inertia and dipole moment of the target, and the mass, charge, and energy of the projectile. A range of these parameters is explored corresponding to collisions at energies above 0.1 eV for most molecules. For large values of the dipole moment, the momentum transfer is much smaller than the prediction of the first-order Born approximation, and involves significant contributions both from elastic scattering and from transitions with large values of $|\Delta j|$. The behavior of the cross section as a function of the rotational quantum number j is found to obey a simple scaling rule.

Appendix G

APPROXIMATE SCALING FORMULA

FOR ION-ION MUTUAL NEUTRALIZATION RATES

A. P. Hickman
Molecular Physics Laboratory
SRI International, Menlo Park, CA 94025

ABSTRACT

A complex potential model is used to treat the mutual neutralization of positive and negative ions. The model is used to examine neutralization by the charge transfer mechanism and also by internal excitation leading to capture. It is found that electron transfer is the dominant process for simple ions and small hydrated ions. The numerical results of the theory have been parameterized in terms of the reduced mass of the collision and the electron affinity of the electron donor. This procedure yields an approximate scaling formula that fits a wide range of experimental data to an accuracy of about $\pm 30\%$.

MP 78-114
11/17/78

I Introduction

This paper concerns the theoretical study of the mutual neutralization reaction between positive and negative ions. This general class of reactions is of the form



where X^+ and Y^- are charged species that may range in size and complexity from simple ions such as H^- , O^- , O_2^+ , NO^+ , or NO_3^- to hydrated or "cluster" ions such as $H_3O^+ \cdot (H_2O)_n$ or $NH_4^+ \cdot (NH_3)_n$. The hydration or cluster number n may range from 1 to 6 or even larger. Typically one of the neutral products of the reaction is in an excited state, denoted in Eq. (1) by X^* . This class of reactions is responsible for the final removal of ions at altitudes below 80 km in the ionosphere, and knowledge of the rate constants is of considerable practical importance.

The purpose of the present work is to develop a model that can be used to estimate rate constants for a wide variety of reactions of the form (1). Two distinct mechanisms will be incorporated into the model. The first is neutralization by electron transfer, which has been previously studied by Olson.¹ Our treatment of electron transfer is similar to Olson's. However, the present theory is more general because it provides a unified framework within which both electron transfer and internal excitation can be treated. Internal excitation has been proposed² as a mechanism leading to a capture reaction and formation of neutral XY. The interaction of the projectile with the target causes a transfer of

energy ΔE from the initial translational mode to internal vibrational and rotational modes. If ΔE is greater than the initial relative kinetic energy, the collision partners will be trapped in a large ellipsoidal orbit. If energy transfer back to translational motion is unlikely, as one would expect when the target is a large cluster, then over a period of several orbits, each successive close encounter will lead to greater internal excitation and a more tightly bound orbit. The ultimate result will be a larger, neutral cluster.

In Section II we develop in detail the theoretical model, which is based on treating the loss of ions to the neutralization channels by adding an imaginary part to the potential. The connection with Olson's absorbing sphere model is discussed. Numerical results are presented and discussed in Section III. Our calculations indicate that electron transfer is the dominant neutralization mechanism for collisions involving small ions and clustered species with $n \leq 3$. The calculations also yield scaling rules for such collisions. We illustrate the effect of single hydration by comparing in detail collisions of $O^- + NO^+$ and $O^- + NO^+ \cdot H_2O$, and discuss qualitatively the application of the model to larger clusters. Section IV contains concluding remarks.

II Theory

A. Complex Potential Model

In this section we develop a complex potential model to treat ion-ion mutual neutralization. We first consider the case of the electron transfer mechanism, and then show how internal excitations can also be included.

A schematic diagram of the relevant potential curves is shown in Figure 1.

The idea is that charge exchange can occur via a curve crossing from the initial ionic potential to any one of a number of closely spaced states of the form $X^* + Y$. It is assumed that the final states are sufficiently closely spaced that at any separation R of X^+ and Y^- , some final state curve will cross the initial state. At this R , the transition occurs predominantly to this particular final state. The matrix element connecting the initial and final states will be denoted by $H_{fi}(R)$. An approximate formula for $H_{fi}(R)$ has been deduced by Olson, Smith, and Bauer³ by correlating a large number of ab initio calculations and experimental results.

Our model consists of treating the closely spaced final states as a continuum, and defining an R -dependent transition probability or width Γ . The function $\Gamma(R)$ gives the rate of transitions out of the initial ionic channel at each R . The dynamics of the collision are treated by adding an imaginary component $- \frac{1}{2} \Gamma(R)$ to the potential function $V(R)$ of the ionic channel. (In the present case, $V(R) = -1/R$). This complex potential model has been used in various other applications⁴⁻⁶ involving an initial state embedded in a continuum of states, and its application to an initial state crossing a series of discrete but closely-spaced states has been discussed by Miller and Morgner.⁷ The general conditions necessary for the validity of the model are the following: 1) The final states must be sufficiently closely spaced that transitions may be considered to occur continuously along a trajectory, rather than at isolated curve crossings; 2) the probability of

transitions from the neutral channels back to the ionic channel must be negligible. We expect these conditions to be valid in the present case.

We now formulate the model more precisely. We define (in the standard way⁸)

$$\Gamma(R) = 2\pi\rho |H_{fi}(R)|^2 \quad (2)$$

ρ is the density of final states. For a manifold of final states whose energy levels are given (in a.u.) by a Rydberg formula

$$E_n = -\frac{1}{2n^2} \quad (3)$$

ρ is easily shown from the work of Miller and Morgner⁷ to be

$$\rho = [2(EA + R^{-1})]^{-\frac{3}{2}} \quad (4)$$

where EA is the electron affinity of Y. We adopt Eq. (4) as the definition of ρ even though the electronic energy levels of a complicated molecule may deviate somewhat from Eq. (3).

The matrix element $H_{fi}(R)$ is defined by Olson, Smith, and Bauer³ and Olson¹ as follows:

$$H_{fi}(R) = 1.044 I_i^{\frac{1}{2}} I_f^{\frac{1}{2}} R^* \exp(-0.857 R^*) \quad (5)$$

where

$$R^* = (I_i^{\frac{1}{2}} + I_f^{\frac{1}{2}})/\sqrt{2} \quad (6)$$

and

$$I_f = I_i + R^{-1} \quad (7)$$

The quantity I_i is the detachment energy (in atomic units) of the electron being transferred. For ground state negative ions, I_i is just the electron affinity EA. Formula (5) is estimated by Olson¹ to be valid to about a factor of three.

The probability of electron transfer on a trajectory whose orbital angular momentum is ℓ is given by⁵

$$P_\ell = 1 - \exp(-2A_\ell) \quad (8)$$

where

$$A_\ell = \int_{R_\ell}^{\infty} \frac{\Gamma(R) dR}{\pi v_\ell(R)} \quad (9)$$

and

$$v_\ell(R) = \left[\frac{2}{m} \left(E + \frac{1}{R} \right) - \frac{(\ell + \frac{1}{2})^2}{2mR^2} \right]^{\frac{1}{2}} \quad (10)$$

In this formula E is the collision energy, and m is the reduced mass. For trajectories in the Coulomb potential, the classical turning point (distance of closest approach) R_ℓ is given by

$$R_\ell = (\ell^2/m) [1 + (1 + 2E\ell^2/m)^{\frac{1}{2}}]^{-1} \quad (11)$$

The total cross section for neutralization is given by

$$\sigma = \frac{\pi}{k^2} \sum_\ell (2\ell + 1) P_\ell \quad (12)$$

where k^2 is related to the collision energy E by $E = \frac{1}{2} k^2 / (2m)$ and to the velocity v by $v = \hbar k / m$. The rate constant α is obtained by taking the appropriate thermal average over a Boltzmann distribution of velocities $f(v, T)$:

$$\alpha(T) = \int_0^{\infty} f(v, T) \sigma(v) v^3 dv \quad (13)$$

where

$$f(v, T) = 4\pi \left(\frac{m}{2\pi kT} \right)^{\frac{3}{2}} \exp\left(-\frac{mv^2}{2kT}\right) \quad (14)$$

For thermal energies, essentially all of the velocity dependence of the cross section Eq. (12) is contained in the $1/k^2$ prefactor. This is because the Coulomb field accelerates particles to velocities many times greater than their initial thermal velocities. To a good approximation, therefore, P_{ℓ} in Eq. (8) may be considered independent of energy, and R_{ℓ} in Eq. (11) may be taken to be

$$R_{\ell} = \ell^2 / 2m \quad (15)$$

Then if $\bar{v} = (8kT/\pi m)^{0.5}$ is the average velocity at temperature T , it is easily shown that

$$\alpha(T) = \frac{4}{\pi} \bar{v} \sigma(\bar{v}) \quad (16)$$

We now consider the extension of the above model to include neutralization via internal excitation of the target. It is necessary to include terms in the potential corresponding to the internal vibration and rotation of the target. We consider here the case that the target has a dipole moment and a single vibrational coordinate. We will treat the rotational and vibrational excitation using the formulas of Semiclassical Perturbation Scattering (SPS) theory.⁹⁻¹¹

In the absence of the electron transfer mechanism, the SPS formulas presented by Miller and Smith¹⁰ may be used to calculate the transition probabilities from the initial state $J j_i \ell_i v_i$ to the final state $J j_f \ell_f v_f$. These are obtained from the T matrix elements, which are written as simple analytic functions of the "average" quantum numbers $J = \frac{1}{2}(j_i + j_f)$, etc., and the changes $\Delta j = (j_f - j_i)$, etc.:

$$T = T(J; \bar{J} \bar{\ell} \bar{v}; \Delta j \Delta \ell \Delta v) \quad (17)$$

Mukherjee and Smith¹¹ showed that the total cross section for a particular $(j_i v_i) \rightarrow (j_f v_i)$ transition is given by

$$\sigma(j_i v_i \rightarrow j_f v_i) =$$

$$\frac{\pi}{k^2(2j_i + 1)} \sum_{\bar{J}} \sum_{\Delta \ell} \sum_{\bar{v}} (2J + 1) |T(J; \bar{J} \bar{\ell} \bar{v}; \Delta j \Delta \ell \Delta v)|^2 \quad (18)$$

where the sum is over values of \bar{J} , $\Delta \ell$, and J consistent with angular momentum conservation. (Explicit limits are given by Mukherjee and Smith.¹¹)

Formula (18) may be written in the form

$$\sigma(j_i v_i \rightarrow j_f v_f) = \frac{\pi}{k^2} \sum_{\bar{L}} (2\bar{L}+1) Q_{\bar{L}} (j_i v_i \rightarrow j_f v_f) \quad (19)$$

where

$$Q_{\bar{L}} (j_i v_i \rightarrow j_f v_f) = \frac{1}{(2j_i+1)(2\bar{L}+1)} \sum_{\Delta j} \sum_J (2J+1) |T(J; \bar{J} \bar{L} \bar{v}; \Delta j \Delta \bar{L} \Delta v)|^2 \quad (20)$$

The similarity of Eq. (19) to Eq. (12) is evident. If one identified \bar{L} with the angular momentum ℓ in the spherically symmetric case, one may interpret $Q_{\bar{L}}$ in Eq. (19) as the probability for a particular (degeneracy averaged) transition on a trajectory whose average orbital angular momentum is \bar{L} .

The preceding formulas for $Q_{\bar{L}}$ and $\sigma(j_i v_i \rightarrow j_f v_f)$ are based on the assumption that electron transfer cannot occur. If we relax this assumption, then a single collision may lead either to electron transfer, or to internal excitation without electron transfer. The cross section for the former process is given as before by Eq. (12). We define the cross section for the latter process by

$$\tilde{\sigma}(j_i v_i \rightarrow j_f v_f) = \frac{\pi}{k^2} \sum_{\bar{L}} (2\bar{L}+1) \tilde{Q}_{\bar{L}} (j_i v_i \rightarrow j_f v_f) \quad (21)$$

where

$$\tilde{Q}_{\bar{L}} (j_i v_i \rightarrow j_f v_f) = (1 - P_{\bar{L}}) Q_{\bar{L}} (j_i v_i \rightarrow j_f v_f) \quad (22)$$

In other words, the probability of internal excitation on a given trajectory depnds on the probability that electron transfer does not occur. This assumption is completely analogous to the assumption frequently made in treating spherically symmetric complex potentials, that the real part of the phase shift does not change as the imaginary part of the potential is "turned on."¹² Such a perturbation assumption is consistent with our use of a perturbation approach to the internal excitation.

Formulas (12) and (21) may be used to calculate cross sections for electron transfer and internal excitation of an ionic polar target. In order to calculate the contribution to the total cross section for neutralization it is necessary to make the further assumption that an internal excitation energy ΔE leads invariably to recombination when $\Delta E > E$ (E is the initial translational energy). This is an excellent approximation as long as there are sufficient internal modes to make an energy transfer back to the translational mode unlikely.

B. Relation to Absorbing Sphere Model

The present complex potential approach may be viewed as a generalization of the absorbing sphere model¹ (ASM). The ASM assumes that if the collision partners approach closer than a certain critical distance R_c , then charge transfer via curve crossing occurs with unit probability. R_c depends on the effective mass m and electron affinity EA , and is the distance at which the matrix element for curve crossing first reaches a particular threshold value. The cross section for neutralization is given by

$$\sigma = \frac{\pi R_c}{E} + \frac{\pi R_c^2}{c} \quad (23)$$

At thermal energies this is well approximated by

$$\sigma \approx \frac{\pi R_c}{E} \quad (24)$$

The complex potential model assigns a neutralization rate (transition probability per unit time) to each value of the coordinate R . The formulas (8)-(12) correspond to integrating this transition probability along the classical trajectories determined by the potential $V(R) = -1/R$. Formula (11) relating the distance of closest approach and the angular momentum of a Coulomb trajectory enables us to compare the results typically obtained for the complex potential model for P_ℓ [Eq. (8)] with the corresponding prediction of the absorbing sphere model. The comparison is shown schematically in Fig. 2. The ASM gives a step function whose discontinuity is at $\ell = (2mR_c)^{1/2}$, whereas the complex potential model tends to smooth out the discontinuity.

The use of an R -dependent transition probability makes the present model somewhat more flexible than the ASM. This flexibility may be especially important when one or both of the ionic species are hydrated. The qualitative discussion in Section III-B shows that the energetics of cluster formation imply that $\Gamma(R)$ should be zero for values of R less than some R^* , where R^* will depend on the size of the cluster. For sufficiently large clusters, R^* may be comparable to R_c . In this case, the probability of neutralization by the curve crossing mechanism would be drastically reduced. For such a large

cluster, one might expect the internal excitation mechanism to be much more important. The complex potential model, with a Γ related to cluster size, provides a consistent framework for examining the collision process as a function of cluster size.

III Results and Discussion

A. Predicted Scaling Behavior

We have found that the results of the complex potential model for a wide variety of systems can be summarized by a simple scaling rule. Here we discuss how this rule was obtained.

It was first determined that the electron transfer mechanism was much more important than internal excitation for simple ions and small clusters. When only the former mechanism is included, the numerical calculation of the rate constant α for any particular system depends only on m and EA . We then sought to express the results of all the numerical calculations by a formula of the form

$$\alpha(T) \propto (T/300 \text{ K})^{-0.5} m^{-0.5} (EA)^\lambda \quad (25)$$

The $T^{-0.5}$ behavior arises whenever the cross section varies as v^{-2} . This behavior was obtained by Olson in the ASM, and was verified in the present case by direct numerical calculation. The $m^{-0.5}$ behavior was also observed in the calculations. It is easily understood by returning to the ASM, which predicts

$$\alpha \sim \bar{v} \sigma(\bar{v}) = \bar{v} \frac{\pi R_c}{E} \quad (26)$$

Since $E \sim \frac{1}{2}mv^2$ and $\bar{v} = (8kT/\pi m)^{0.5}$,

$$\alpha \propto \frac{R_c}{m^{0.5} T^{0.5}} \quad (27)$$

However, our examination of the absorbing sphere model has shown that R_c depends most strongly on EA, and only logarithmically on m. We therefore expect that the dependence of α on m and EA might be approximated by a power law as in Eq. (25). If this formula is reasonable, then a log-log plot of $\alpha m^{0.5}$ (at $T = 300$ K) vs EA will give a straight line of slope λ . Fig. 3 shows that such a plot is nearly linear. The slope is determined by a least squares fit to be $\lambda = -0.4$. We therefore obtain the following formula

$$\alpha^{-1} = C(T/300 \text{ K})^{0.5} m^{0.5} (\text{EA})^{0.4} \quad (28)$$

If the units of α , m, and EA are cm^3/sec , a.u., and eV, respectively, then $C = 4.38 \times 10^4$.

Figure 4 and Table II show that Eq. (28) provides a simple correlation of a wide range of data.¹³⁻¹⁷ Considering that the basic formula for $H_{fi}(R)$ was only expected to be accurate to a factor of three, and that the data range from collisions of H^+ and H^- to $H_3O^+ \cdot (H_2O)_3$ and NO_3^- , the approximate scaling rule must be considered remarkably successful.

B. Qualitative Discussion of the Effects of Clustering

The energetics of cluster formation have been previously discussed,² and in some cases quantitative calculations have been carried out.^{18,19} This section discusses the application of the complex potential model to larger clusters.

In general, one expects that the addition of successive waters of hydration will lower the energy of the ion pair state relative to the corresponding neutrals.² The situation is illustrated by the schematic diagram in Fig. 5. The energy of $X^+ \cdot H_2O$ is lower than that of X^+ and an infinitely separated H_2O because of the charge-dipole and polarization interactions. In contrast, one expects the energy of $X^* \cdot H_2O$, at the equilibrium separation of $X^+ \cdot H_2O$, to be slightly higher than the energy of X^* .

The curve $X + Y^*$ in Fig. 5 denotes the lowest state to which charge transfer can occur. Because of the stabilizing effect of clustering, discussed in the preceding paragraph, this asymptote moves closer and closer to the ionic state as the cluster size increases. In the context of the complex potential model, we may interpret this to mean that $\Gamma(R)$ should be nonzero only for $R \geq R^*$. An estimate previously used is that each water of hydration moves the two asymptotes 1 eV closer together.² If this is the case, then R^* is given (in a.u.) by

$$1/R^* = W - n/27.2 \quad (29)$$

n is the hydration number, and W is the energy difference (in a.u.) between the asymptotes $X^- + Y^+$ and $X + Y^*$, and may be crudely estimated by

$$W \approx IP(Y) - EA(X) \quad (30)$$

that is, the difference between the ionization potential of Y

and the electron affinity of X. For many species of atmospheric interest, W is in the range 6-8 eV (0.2-0.3 a.u.).

Trial calculations were performed in which $\Gamma(R)$ was set to zero for $R \leq R^* = 10 a_0$. The change in the rate constant was negligible (less than 1%), indicating that electron transfer occurs mainly at large R. It is likely that cluster formation would cause a reduction in the matrix element for electron transfer. We found that reducing $\Gamma(R)$ by a factor of four caused only about a 25% decrease in the rate constant. Combined with Eq. (29) and our estimate of W, these results suggest that for small clusters ($n \leq 3$), hydration does not significantly inhibit electron transfer.

C. The Internal Excitation Mechanism: Calculations for $O^- + NO^+$
and $O^- + NO^+ \cdot H_2O$

The system $O^- + NO^+$ is particularly well suited to the application of the complex potential model because the real part of the potential, both the isotropic and anisotropic parts, can be modelled asymptotically using the dipole moment function²⁰ of NO^+ . Cross sections for rotational and vibrational excitation have been calculated both with and without the imaginary part of the potential, using Semiclassical Perturbation Scattering (SPS) theory. The application of this theory in the case where the dipole moment is a linear function of the vibrational coordinate has been discussed by Miller and Smith.¹⁰ Furthermore, we have constructed a simple model for the geometry of $NO^+ \cdot H_2O$, and have examined the cross sections for excitation of the lowest frequency rotational and vibrational modes. The results allow

us to examine the competition between the electron transfer and the internal excitation mechanisms for simple ions, and also to obtain information about the changes that occur with the first hydration.

Figure 6 shows the assumed geometry of the $\text{NO}^+ \cdot \text{H}_2\text{O}$ complex. For simplicity, we assume that the center of charge is at the midpoint of the NO^+ , and that the interaction of the oxygen of the water molecule with the N and the other O can be described by a Born-Mayer potential²¹ of the form

$$f(X) = A \exp(-BX) \quad (31)$$

where $A = 74.445$ a.u. and $B = 2.006$ a.u. This potential is the geometric mean of the Born-Mayer potentials for neutral O-N and O-O interactions. The internuclear separation of NO^+ is taken to be the unperturbed value $2a = 2.00$ a._o. With these assumptions, the equilibrium geometry will have $\theta = \pi/2$, and R can be determined from the minimum value of the interaction

$$V(R) = 2A \exp[-2B(R^2 + a^2)^{1/2}] - \frac{\mu_0 e}{R^2} \quad (32)$$

where $\mu_0 = 1.85$ D = 0.728 a.u. is the dipole moment of H_2O . For these values of the parameters, the equilibrium value of R is 4.9 a.u., and the well depth is 0.65 eV.

The above model allows us to calculate the dipole moment (relative to the center of mass), moment of inertia, and rotational energy level spacing of $\text{NO}^+ \cdot \text{H}_2\text{O}$, treating it as a rigid linear molecule. These values are summarized in Table I. The model also allows us to estimate the frequencies of the lowest vibrational or bending modes, and to obtain the dependence of

the dipole moment function on the corresponding internal coordinates. We consider both vibration in the R coordinate and bending in the θ coordinate. Estimated frequencies for these modes, assuming they are uncoupled, are also given in Table I.

The results of our calculations may be summarized as follows. For $O^- + NO^+$, the electron transfer mechanism dominates the scattering. Any trajectory that would lead to significant rotational or vibrational excitation in the absence of the width Γ , has a high probability (essentially unity) of electron transfer when Γ is turned on. Also, for those trajectories where the electron transfer probability is small (i.e., large δ or large classical turning point), vibrational excitation is much less important than rotational excitation and may be neglected. We have also found that electron transfer is the most important mechanism for $O^- + NC^+ \cdot H_2O$, but that internal excitation may increase the rate constant by about 10% at 300 K. The reason for this is that the cluster has a larger dipole moment than the bare NO^+ , and hence rotational excitation can occur for more distant trajectories than for NO^+ alone. The calculations showed that the cross sections for vibrational excitation were considerably smaller than those for rotational excitation for all trajectories not leading to electron transfer. In other words, for the purposes of the complex potential model, the singly hydrated cluster behaves as if it were a rigid rotor.

The final rate constants obtained were as follows. For $O^- + NO^+$, $\alpha (300 \text{ K}) = 13.9 \times 10^{-18} \text{ cm}^3/\text{sec}$, essentially all from electron transfer.

For $O^- + NO^+ \cdot H_2O$, the rate constant from electron transfer is α (300 K) = $13.1 \times 10^{-8} \text{ cm}^3/\text{sec}$; the inclusion of internal excitation changes this to $14.1 \times 10^{-8} \text{ cm}^3/\text{sec}$.

The extension of the present model, with its detailed assumptions about geometry, to larger clusters is probably not justified without rigorous structure calculations. A few general comments may be pertinent, however. The addition of more water molecules will probably decrease, not increase, the total dipole moment, since some cancellation could be expected to occur. This suggests that large rotational excitation due to distant trajectories may be important only for single (or un-)hydrated ions. The large clusters will have a greater number of internal modes that can be excited by direct impact. Previous discussion has indicated that electron transfer may not occur at close distances for these larger clusters. It may be that at small distances neutralization occurs instead with high probability by the internal excitation mechanism.

IV Conclusions

We have presented a theory of ion-ion mutual recombination based on modelling the loss of particles from the initial channel to a manifold of final channel by adding an imaginary part to the Coulomb potential. We have examined the relative importance of competing mechanisms, and have found that the electron transfer process accounts for at least 80% of the rate constant in the cases considered. The results of the theory have been parameterized, and provide a useful and reasonably accurate correlation of a wide range of experimental data.

This correlation formula, Eq. (28), predicts a small decrease in the neutralization rate as the size of the positive ion cluster increases. This effect is due entirely to the change in the effective mass of the relative motion. However, our more detailed study of collisions of hydrated NO^+ with O^- showed a net increase in the rate as the hydration number increased from zero to one, because of the increased probability of internal excitation. It is felt that these results cannot be interpreted to indicate any general trend of neutralization rates as a function of cluster size. They appear only to suggest that the rates for small clusters are not substantially different from the rates for the corresponding bare ions.

Acknowledgments

The author wishes to acknowledge helpful conversations with D. L. Huestis, J. R. Peterson, R. E. Olson, and F. T. Smith. This research was supported by the Defense Nuclear Agency under Subtask No. S99QAXHD411, Reaction Rates Essential to Propagation through the Air Force Geophysics Laboratory under Contract No. F19628-75-C-0050.

REFERENCES

1. R. E. Olson, *J. Chem. Phys.* 56, 2979 (1972).
2. R. A. Bennett, D. L. Huestis, J. T. Moseley, D. Mukherjee, R. E. Olson, S. W. Benson, J. R. Peterson, and F. T. Smith, *ARCRL-TR-74-0417*, Air Force Cambridge Research Laboratory, Hanscom, MA, 1974 (unpublished).
3. R. E. Olson, F. T. Smith, and E. Bauer, *Appl. Opt.* 10, 1848 (1971).
4. N. F. Mott and H.S.W. Massey, *The Theory of Atomic Collisions*, Third Edition (Clarendon Press, Oxford, 1965), pp. 184-186.
5. W. H. Miller, *J. Chem. Phys.* 52, 3563 (1970).
6. A. P. Hickman and H. Morgner, *J. Phys. B: Atom. Molec. Phys.* 9, 1765 (1976).
7. W. H. Miller and H. Morgner, *J. Chem. Phys.* 67, 4923 (1977).
8. W. H. Miller, *Chem. Phys. Lett.* 4, 627 (1970).
9. F. T. Smith, D. L. Huestis, D. Mukherjee, and W. H. Miller, *Phys. Rev. Lett.* 35, 1073 (1975).
10. W. H. Miller and F. T. Smith, *Phys. Rev. A* 17, 939 (1978).
11. D. Mukherjee and F. T. Smith, *Phys. Rev. A* 17, 954 (1978).
12. Z. F. Wang, A. P. Hickman, K. Shobatake, and Y. T. Lee, *J. Chem. Phys.* 65, 1250 (1976).
13. J. R. Peterson, W. H. Aberth, J. T. Moseley, and J. R. Sheridan, *Phys. Rev. A* 3, 1651 (1971).
14. W. H. Aberth and J. R. Peterson, *Phys. Rev. A* 1, 158 (1970).

15. J. T. Moseley, W. H. Aberth, and J. R. Peterson, *J. Geophys. Res.* 77, 255 (1972).
16. D. Smith, M. J. Church, and T. M. Miller, *J. Chem. Phys.* 68, 1224 (1978).
17. J. T. Moseley, R. E. Olson, and J. R. Peterson, *Case Studies in Atomic Physics* 5, 1 (1975).
18. M. D. Newton and S. Ehrenson, *J. Am. Chem. Soc.* 93, 4971 (1971).
19. M. D. Newton, *J. Chem. Phys.* 67, 5535 (1977).
20. F. P. Billingsley, *Chem. Phys. Lett.* 23, 160 (1973).
21. A. A. Abrahamson, *Phys. Rev.* 178, 76 (1969).

Table I. Values of the molecular parameters of NO^+ and $\text{NO}^+\cdot\text{H}_2\text{O}$ used in the calculations. Note that the vibrational coordinate of NO^+ is the N-O distance; that of $\text{NO}^+\cdot\text{H}_2\text{O}$ is the coordinate R shown in Fig. 6, with NO at its equilibrium value.

Parameter	NO^+	$\text{NO}^+\cdot\text{H}_2\text{O}$
Rotational constant (cm^{-1})	1.99	0.22
Moment of inertia (gm cm^2)	1.465×10^{-39}	1.29×10^{-38}
Equilibrium value of vibrational coordinate, R_o (a.u.)	2.0	4.9
Well depth (eV)		0.65
Equilibrium value of dipole moment relative to c.m., $\mu_o = \mu(R_o)$, (a.u.)	0.313	1.13
Dipole derivative $\mu'(R_o)$ (a.u.)	0.392	0.375
Vibrational Frequency (a.u.) ω_v	0.011	$\sim 9.1 \times 10^{-4}$
Bending Frequency (a.u.) ω_b		$\sim 2.1 \times 10^{-4}$

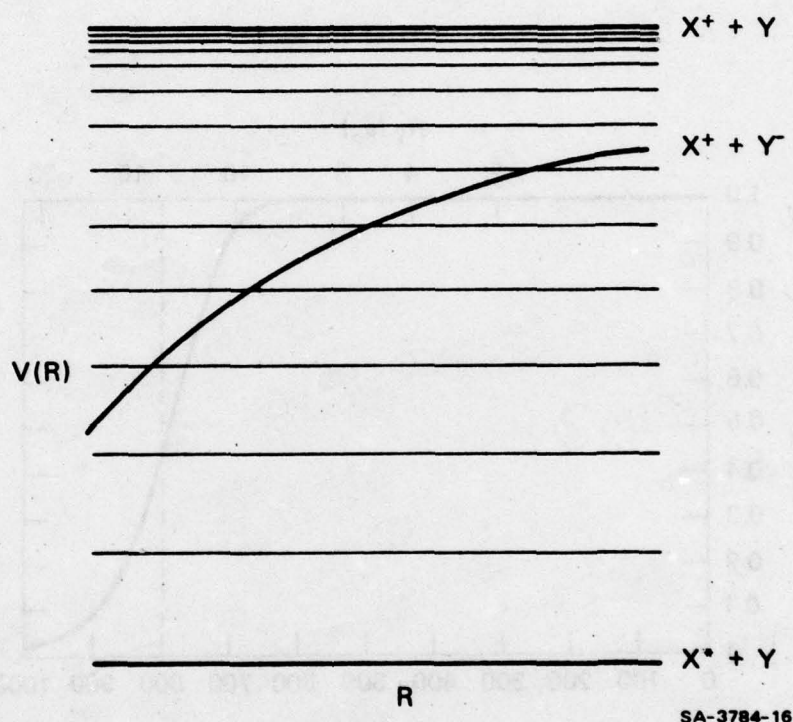
Table II. Details of the experimental data

plotted in Figure 4. Units are as in Fig. 4.

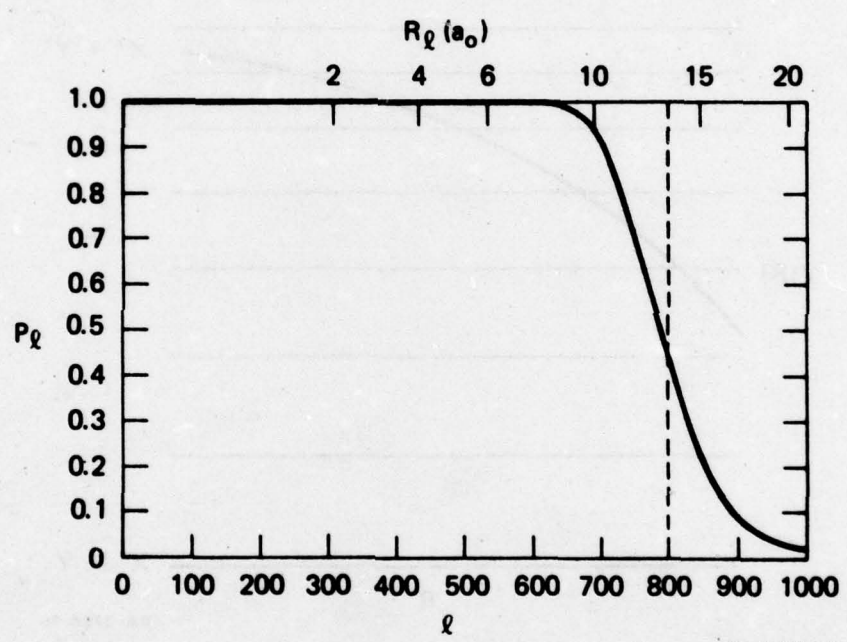
Ions	$m^{0.5}$ (EA) ^{0.4}	α	Reference
$H^+ + H^-$	27	39 ± 21	13
$H_2^+ + D^-$	38	47 ± 15	17
$N_2^+ + O_2^-$	118	16 ± 5	14
$H^+ + O^-$	137	26 ± 8	13
$O^+ + O^-$	142	27 ± 13	13
$Na^+ + O^-$	153	21 ± 10	15
$NO^+ + O^-$	162	49 ± 20	15
$O_2^+ + O^-$	164	10 ± 4	15
$NO^+ + NO_2^-$	232	6.4 ± 0.7	16
$NH_4^+ + Cl^-$	247	6.7 ± 0.7	16
$NH_4^+ \cdot (NH_3)_2 + NO_2^-$	270	4.9 ± 0.6	16
$NO^+ + NO_3^-$	278	5.7 ± 0.6	16
$NH_4^+ \cdot (NH_3)_2 + Cl^-$	329	7.9 ± 1.0	16
$H_2O^+ \cdot (H_2O)_3 + Cl^-$	350	4.8 ± 0.6	16
$H_3O^+ \cdot (H_2O)_3 + NO_3^-$	356	5.5 ± 1.0	16
$CClF_2^+ + Cl^-$	359	4.1 ± 0.4	16
$CCl_3^+ + Cl^-$	375	4.5 ± 0.5	16

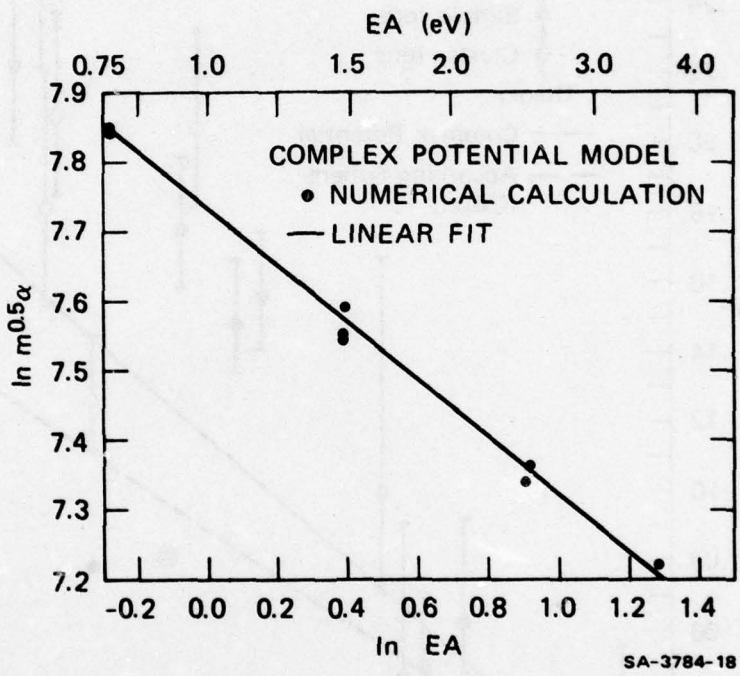
Figure Captions

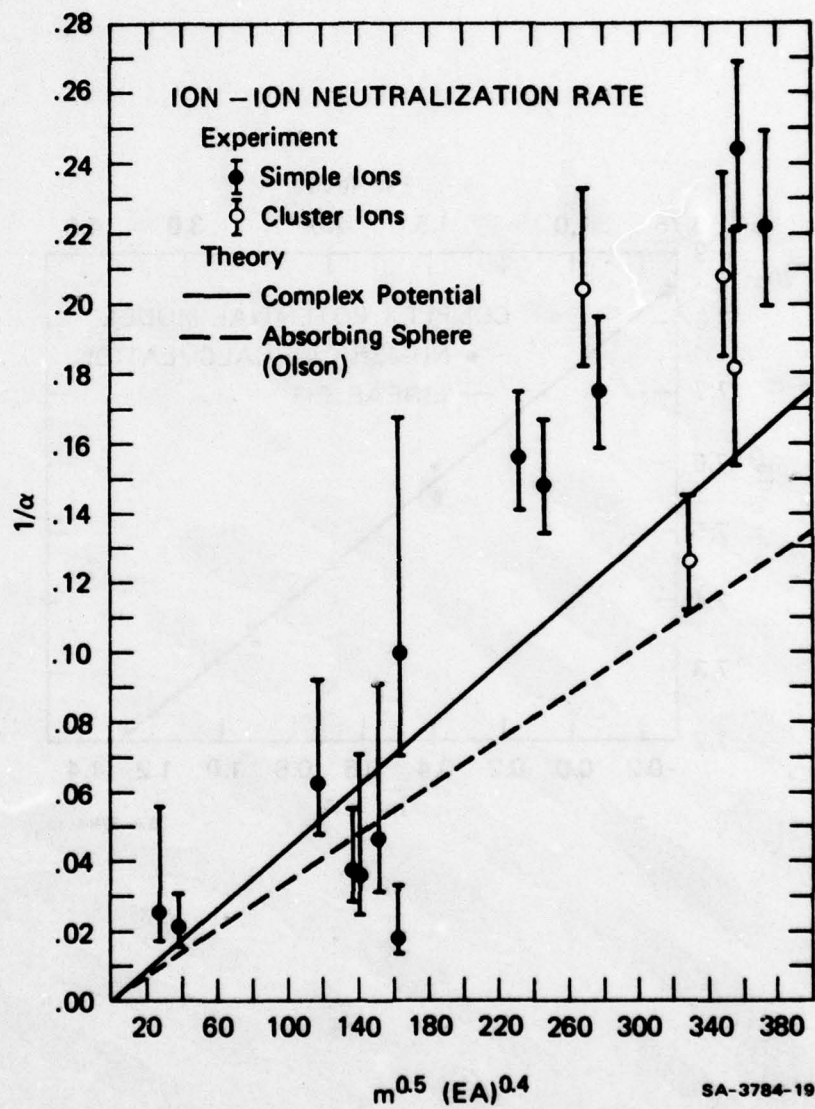
1. Schematic diagram of the relevant potential curves for ion-ion mutual neutralization. The state $X^* + Y$ is one of a manifold of closely spaced states indicated by the light lines.
2. Schematic illustration of the neutralization probability as a function of orbital angular momentum ℓ or classical turning point $R_\ell = \ell^2/2m$, for the complex potential model (solid line) and the absorbing sphere model (dashed line).
3. Demonstration that the numerical results of the complex potential model (points) may be approximately fit by a straight line on an appropriate log-log plot, leading to the power law dependence of Eqs. (25) and (28). EA is given in eV, m in a.u., and α in $10^{-8} \text{ cm}^3/\text{sec.}$
4. Comparison of the scaling law, Eq. (28), and experimental data. α is calculated at $T = 300 \text{ K}$. EA is given in eV, m in a.u., and α in $10^{-8} \text{ cm}^3/\text{sec.}$ The data is tabulated for reference in Table II.
5. Schematic diagram showing how hydration tends to lower the energy of an ion pair state relative to the corresponding neutrals. In the text it is argued that for $R < R^*$, $\Gamma(R)$ should be zero.
6. The geometry assumed for a simple model of $\text{NO}^+ \cdot \text{H}_2\text{O}$. The diagram is not to scale.

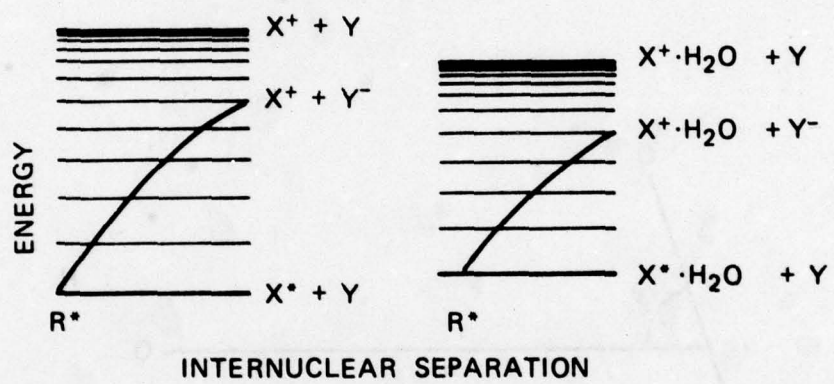


SA-3784-16

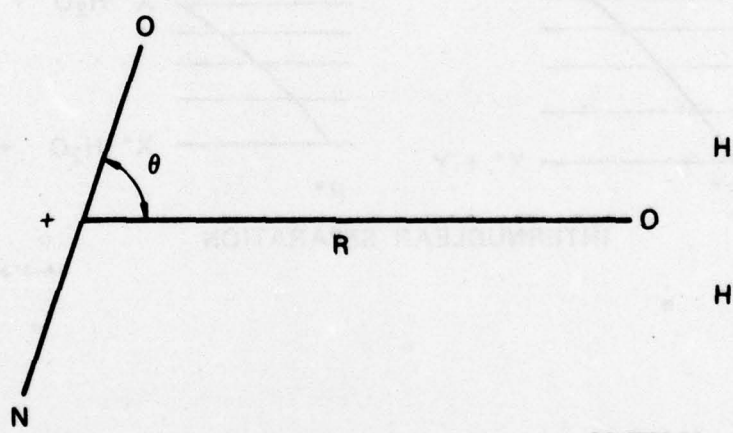








SA-3784-20



SA-3784-21

DNA Distribution List

Department of Defense

Director
Defense Advanced Research Projects Agency
1400 Wilson Boulevard
Arlington, VA 22209

1 cy ATTN: TIO
1 cy ATTN: STO
1 cy ATTN: NRMO

Director
Defense Communications Agency
8th Street and Courthouse Road
Arlington, VA 22204

3 cys ATTN: MEECN Office

Defense Documentation Center
Cameron Station
Alexandria, VA 22314

12 cys ATTN: TC

Director
Defense Nuclear Agency
Washington, D. C. 20305

1 cy ATTN: STTL
1 cy ATTN: DDST
3 cys ATTN: RAAE
1 cy ATTN: RAEV

Department of Defense (Continued)

Joint Chiefs of Staff
Department of Defense
Washington, D. C. 20301

1 cy ATTN: J-6

Director
National Security Agency
Fort George G. Meade, MD 20755

2 cys ATTN: Technical Library

Under Secretary of Defense (Research and Engineering)
Department of Defense
Washington, D. C. 20301

2 cys ATTN: DDS&SS

Department of Commerce

U. S. Department of Commerce
Office of Telecommunications
Institute for Telecommunication Sciences
National Telecommunications and Information Administration
Boulder, CO 80303

2 cys ATTN: W. F. Utlaut

Department of the Army

Commander/Director
Atmospheric Sciences Laboratory
U. S. Army Electronics Command
White Sands Missile Range, NM 88002

1 cy ATTN: DRSEL-BL-SY-S
F. E. Niles

Director
U. S. Army Ballistic Research Laboratories
Aberdeen Proving Grounds, MD 21005

1 cy ATTN: George E. Keller

Commander
U. S. Army Foreign Sciences and Technology Center
220 7th Street, N.E.
Charlottesville, VA 22901

1 cy ATTN: Robert Jones

Department of the Navy

Chief of Naval Operations
Department of the Navy
Washington, D.C. 20350

1 cy ATTN: NOP 985
1 cy ATTN: NOP 094H

Department of the Navy (Continued)

Chief of Naval Research
Department of the Navy
800 North Quincy Street
Arlington, VA 22217

1 cy ATTN: Code 465, R. G. Joiner
1 cy ATTN: Code 427, H. Mullaney

Commander
Naval Electronic Systems Command
Department of the Navy
Washington, D.C. 20360

1 cy ATTN: PME-117
1 cy ATTN: PME-117T
1 cy ATTN: PME-117-21
1 cy ATTN: PME-117-21A
1 cy ATTN: PME-117-22

Director
Naval Ocean Systems Center
Electromagnetic Propagation Division
271 Catalina Boulevard
San Diego, CA 92152

1 cy ATTN: Code 2200, W. F. Moler
1 cy ATTN: Code 2200, Ilan Rothmuller
1 cy ATTN: Code 2200, John Bickel

Director
Naval Research Laboratory
4555 Overlook Avenue, S.W.
Washington, D.C. 20375

1 cy ATTN: Code 7700, Timothy P. Coffey
1 cy ATTN: Code 7709, Wahab Ali
2 cys ATTN: Code 7750, John Davis
1 cy ATTN: Code 2627

Commander
Naval Surface Weapons Center (White Oak)
Silver Spring, MD 20910

1 cy ATTN: Technical Library

Office of Naval Research Branch Office
1030 East Green Street
Pasadena, CA 91106

1 cy

Department of the Air Force

Commander

Air Force Geophysical Laboratory, AFSC
L. G. Hanscom Air Force Base, MA 01731

1 cy ATTN: OPR, James Ulwick
1 cy ATTN: LKB, W. Swider
1 cy ATTN: LKB, K. Champion

Director

Air Force Technical Applications Center
Patrick Air Force Base, FL 32920

1 cy ATTN: TD
1 cy ATTN: HQ 1035th TCHOG/TFS

Department of Defense Contractors

General Electric Company
TEMPO - Center for Advanced Studies
816 State Street
Santa Barbara, CA 93102

1 cy ATTN: Warren S. Knapp
1 cy ATTN: DASIAC

Lockheed Missiles and Space Company
3251 Hanover Street
Palo Alto, CA 94304

1 cy ATTN: J. B. Reagan
1 cy ATTN: W. Imhof
1 cy ATTN: Martin Walt

Mission Research Corporation
735 State Street
Santa Barbara, CA 93101

1 cy ATTN: M. Scheibe
1 cy ATTN: D. Sowle

Pacific-Sierra Research Corporation
1456 Cloverfield Boulevard
Santa Monica, CA 90404

1 cy ATTN: E. C. Field

Pennsylvania State University
Ionospheric Research Laboratory
College of Engineering
318 Electrical Engineering - East Wing
University Park, PA 16802

1 cy ATTN: John S. Nisbet
1 cy ATTN: Les Hale
1 cy ATTN: A. J. Ferraro
1 cy ATTN: H. S. Lee

1000 Admiralty Way
Marina Del Rey, CA 90291

1 cy ATTN: R. Lelevier
1 cy ATTN: F. Gilmore
1 cy ATTN: R. Turco

The Rand Corporation
1700 Main Street
Santa Monica, CA 90406

1 cy ATTN: Cullen Crain

Professor Chalmers F. Sechrist
155 Electrical Engineering Building
University of Illinois
Urbana, IL 61801

1 cy ATTN: C. Sechrist

Stanford Research Institute
333 Ravenswood Avenue
Menlo Park, CA 94025

1 cy ATTN: Allen M. Peterson
1 cy ATTN: Ray L. Leadabrand

University of Pittsburgh
Dept. of Physics & Astronomy
Pittsburgh, PA. 15260

1 cy ATTN: M.A.Biondi
1 cy ATTN: F.Kaufman
1 cy ATTN: W.Fite

General Electric CO. , Space Division, VFSC
Goddard Blvd., King of Prussia
P.O.Box 8555
Philadelphia, PA 19101

1 cy ATTN: M.H.Bortner
1 cy ATTN: T.Baurer

National Oceanic & Atmospheric Admin.
Environmental Research Laboratories
Dept. of Commerce
Boulder, CO 80302

1 cy ATTN: E.E.Ferguson
1 cy ATTN: F.Fehsenfeld